Accepted Manuscript

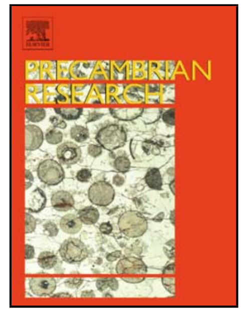


Title: The 1375 Ma ”Kibaran Event” in Central Africa: prominent emplacement of bimodal magmatism under extensional regime

Authors: L. Tack, M.T.D. Wingate, B. De Waele, J. Meert, E. Belousova, B. Griffin, A. Tahon, M. Fernandez-Alonso

PII: S0301-9268(10)00063-X
DOI: doi:10.1016/j.precamres.2010.02.022
Reference: PRECAM 3208

To appear in: *Precambrian Research*

Received date: 30-6-2009
Revised date: 15-2-2010
Accepted date: 22-2-2010

Please cite this article as: Tack, L., Wingate, M.T.D., De Waele, B., Meert, J., Belousova, E., Griffin, B., Tahon, A., Fernandez-Alonso, M., The 1375 Ma ”Kibaran Event” in Central Africa: prominent emplacement of bimodal magmatism under extensional regime, *Precambrian Research* (2008), doi:10.1016/j.precamres.2010.02.022

# The 1375 Ma "Kibaran Event" in Central Africa: prominent emplacement of bimodal magmatism under extensional regime

L. Tack[1]*, M.T.D. Wingate[2/3], B. De Waele[4], J. Meert[5], E. Belousova[6], B. Griffin[6], A. Tahon[1] and M. Fernandez-Alonso[1]

[1]Department of Geology and Mineralogy, Royal Museum for Central Africa (RMCA), 3080 Tervuren, Belgium; e-mail: luc.tack@africamuseum.be
[2]Geological Survey of Western Australia, 100 Plain Street, East Perth, WA 6004, Australia
[3]Tectonics Special Research Centre, School of Earth and Environment, University of Western Australia, Perth, Australia
[4]SRK Consulting, 10 Richardson Street, West Perth, WA 6005, Australia
[5]Department of Geological Sciences, University of Florida, 241 Williamson Hall, Gainesville, FL 32611 USA
[6]GEMOC, Department of Earth and Planetary Sciences, Macquarie University, NSW, Australia

*corresponding author:

Luc Tack
Department of Geology and Mineralogy
Royal Museum for Central Africa
Leuvensesteenweg 13
B. 3080 Tervuren
Belgium
e-mail: luc.tack@africamuseum.be

## ABSTRACT

In previous literature, the "Kibara belt" has often been portrayed as a Mesoproterozoic belt trending NE over 1300 km across the Central African Congo craton, from the Angola-Zambia-D.R.Congo border triple-junction in the SW, through Katanga and Kivu-Maniema (DRC), Rwanda and Burundi, up to SW Uganda and NW Tanzania in the NE. However, north of Katanga in the DRC, there is a clear break in continuity of the thus-defined "Kibara belt", cross-cut by Palaeoproterozoic (Rusizian) terranes, in structural continuity with the NW-SE trending Ubende shear belt further south in Tanzania.

In this paper, we redefine the use of the term “Kibara belt” (“KIB”), restricting it henceforward to the belt occurring SW of the Ubende-Rusizian terranes, i.e. in the Kibara Mountains type area of Katanga (DRC). The other belt situated NE of the Ubende-Rusizian terranes and east of the Western Rift, previously referred to as  the “Northeastern Kibaran Belt” (NKB), is henceforward and for clarity reasons re-named “Karagwe-Ankole belt” (“KAB”). In our re-definitions, we do not take into account the Kivu-Maniema (DRC), because of its geological complexity apparent from satellite imagery and the lack of recent field data, although “some continuity” of the KAB in Kivu-Maniema is obvious.

For the KAB, we document 10 new SHRIMP U-Pb zircon ages, in addition to new $^{40}Ar/^{39}Ar$ and laser-ablation zircon Hf data, all of them obtained from previously already isotopically “dated” rock specimens. Contrary to previous belief, magmatism in the KAB (and the KIB) is punctuated by the profuse emplacement of bimodal intrusions between 1380 and 1370 Ma. Moreover, the occurrence of Palaeoproterozoic basement within the KAB is confirmed. The prominent c. 1375 Ma bimodal magmatism in the KAB consists of 1) the 350 km long Kabanga-Musongati (KM) alignment of mafic and ultramafic, Bushveld-type, layered complexes, originating from an enriched lithospheric mantle source and 2) voluminous S-type granitoid rocks with accompanying subordinate mafic intrusive rocks. Both coeval magmatic suites are interpreted to have been emplaced under extensional regime in a regional-scale intra-cratonic setting. During ascent the mantle-derived magmas have taken advantage of the regionally occurring crustal-scale zone of weakness in the KAB, i.e. the rheological boundary between the Archaean craton of Tanzania, to the east, and the adjacent Palaeoproterozoic basement (2.1 Ga mobile belt), to the west, both overlain by Mesoproterozoic (meta)sedimentary rocks. The mantle-derived magmas initiated concomittantly and under extension, large-scale crustal melting preferentially of the Palaeoproterozoic basement, and characterized by the absence of a thick lithospheric profile in contrast to the nearby Archaean craton. Such petrogenetic processes have intra-plate characteristics and are thus not associated with normal plate boundary processes nor with their typical magmatism. On the contrary, they may include rift-related packages, characteristically associated with successful or attempted, though unsuccessful, continental break-up as was the case here.

In the KAB, later magmatic events occurred respectively at c. 1205 (A-type granitoids) and c. 986 Ma ("tin-granites"). They represent minor additions to the crust.

For decades the term "Kibaran" has been used to name the orogenic cycle and/or orogeny occurring in (Central) Africa in "late" Mesoproterozoic times (1.4-1.0 Ga), which was considered to have a protracted character. Here, we propose to restrict henceforward the term "Kibaran" only to the prominent tectono-magmatic "event", giving rise to the coeval c. 1375 Ma bimodal magmatism emplaced under extensional regime. This "Kibaran event" pre-dates compressional deformation, reflecting far-field effects of global orogenic events, external to the craton and possibly related to Rodinia amalgamation.

**KEYWORDS:** Karagwe-Ankole belt (KAB), Kibara belt (KIB), Mesoproterozoic, coeval bimodal magmatism, 1375 Ma Kibaran event, Central Africa

## INTRODUCTION AND NEW (RE)DEFINITIONS

The "Kibara belt" (or "Kibaran belt") of Central Africa is defined in existing literature as a belt of Mesoproterozoic supracrustal units, mostly metasedimentary rocks and minor metavolcanic rocks, intruded by voluminous S-type granitoid massifs and subordinate mafic bodies, also of Mesoproterozoic age (Cahen et al., 1984 and references therein). It has often been portrayed as a single, continuous orogenic belt that trends NE over some 1300 km from the Katanga region in the Democratic Republic of Congo (DRC) up to the Ankole region in SW Uganda (Fig. 1a, see box after Brinckmann et al., 2001; see also e.g. Kokonyangi et al., 2006; Buchwaldt et al., 2008).

However, from satellite imagery and derived products (e.g. Landsat, SRTM DEM ), it is evident that there is a break in continuity of the thus-defined "Kibara belt". Indeed, the latter is "cross-cut" by the NW-trending Palaeoproterozoic Ubende belt of SW Tanzania extending along trend across Lake Tanganyika into the Kivu-Maniema region of the DRC (Fig. 1b). There it has been mapped as Palaeoproterozoic "Rusizian" basement (e.g. Cahen and Snelling, 1966; Lepersonne, 1974; Lavreau, 1985; Fig. 1a). In the last fifty years, only limited fieldwork has been conducted in this structurally complex DRC region (Walemba, 2001; Rumvegeri et al., 2004; Villeneuve and Guyonnet-Benaize, 2006 and references therein).

The apparent paradox of Palaeoproterozoic "Ubende-Rusizian terranes" cross-cutting the Mesoproterozoic "Kibara belt" results from repeated crustal-scale structural reactivation along the Ubende-Rusizian terranes (Klerkx et al., 1998 and references therein). Indeed, the Ubende belt itself consists of 2100-2025 Ma high-grade protolith (Theunissen et al., 1996), exhumed under amphibolite-facies conditions in the 1950-1850 Ma time interval (Boven et al., 1999).

Previous attempts at reconstructing the orogenic history of the "Kibara belt" relied mostly on Rb-Sr and K-Ar whole-rock and mineral ages, and only a few bulk zircon ages (Cahen et al., 1984; Pohl, 1994). Klerkx et al. (1984, 1987) envisaged a protracted, intra-cratonic orogeny with successive extensional and compressional phases, characterised by the intrusion of pulses of S-type granitoid magma between c. 1330 and 1180 Ma (whole-rock Rb-Sr dating). The same multi-phase time frame was adopted by Kampunzu et al. (1986), Rumvegeri (1991) and Rumvegeri et al. (2004), who viewed the "Kibaran orogeny" in a subduction-collision setting. Tack et al. (1994) proposed a model that involved delamination of continental lithospheric mantle and late-orogenic extensional collapse, based on petrological studies of A-type granitoids and of mafic and ultramafic rocks, including two bulk zircon ages. Fernandez-Alonso and Theunissen (1998) advocated an intra-cratonic extensional detachment model, conditioned by strike-slip reactivation (Theunissen, 1988, 1989) of NW-trending shear zones in Palaeoproterozoic basement, timed according to the multi-phase framework of Klerkx et al. (1984, 1987).

The world-scale Central African Sn-Nb-Ta-W and Au metallogenic province, which was formed by the c. 970 Ma emplacement of Sn-bearing granites and associated mineralisation hosted in pegmatites and/or quartz veins (Cahen et al., 1984; Ikingura et al., 1992; Pohl, 1994; Romer and Lehmann, 1995; Dewaele et al., 2007a, b, 2008) coincides with portions of the "Kibara belt".

There is proficient confusion in literature with the descriptive term "Kibara belt" and what it stands for. "Synonyms" like Kibaran belt, Kibara belt sensu lato, Kibara belt sensu stricto and Northeastern Kibaran Belt (NKB) have been used depending upon the fact that authors took into account or not the hereabove explained cross-cutting relationships in the "Kibara belt".

For the sake of clarity, we will use henceforward the name "Kibara belt" ("KIB") only for the part occurring SW of the Ubende belt - Rusizian basement extension, i.e. in the Katanga region of the DRC, which includes the Kibara Mountains type area (Fig. 1a). For the part to the NE of this extension, and east of the Western Rift - in line with our contention that this part is distinct from the KIB as just redefined hereabove - we adopt on the basis of nomenclature precedence the name "Karagwe-Ankole belt" ("KAB") (Fig. 1a). This name has been used historically to designate the Mesoproterozoic belt in respectively the Karagwe (NW Tanzania) and Ankole (SW Uganda) regions (see Cahen et al., 1984, and references therein). The KAB corresponds to the NKB as defined by Tack et al. (1994). In view of the lack of recent field data and the stratigraphic and structural complexity that is apparent from satellite imagery, the Kivu-Maniema (DRC) region, north of the Ubende belt – Rusizian basement extension and west of the Western Rift, is left undefined for now although "some continuity" of the KAB in Kivu-Maniema is obvious but not a topic of the present article.

Following the above reformulated definitions, the terms "Kibara belt" (KIB) and "Karagwe-Ankole belt" (KAB) – written as proper name and not as adjective – will be used henceforward in a purely descriptive and geographic sense (Fig. 1a).

In this paper, we present new Sensitive High Resolution Ion Microprobe (SHRIMP) U-Pb zircon ages, $^{40}Ar/^{39}Ar$ and laser-ablation zircon Hf data for the KAB, which shed new light on the evolution of the latter during the Meso-Neoproterozoic.

A companion-paper (Fernandez-Alonso et al., in prep.) is devoted to new data pertaining to the evolution of the sedimentary basin of the KAB, including the GIS-based geological compilation map with revised, belt-wide lithostratigraphy (see also Fernandez-Alonso, 2007) and provenance analysis data obtained from SHRIMP on detrital zircons. The paper also reviews the Proterozoic intra-cratonic history under extensional and/or compressional regimes of both the KAB and the KIB (Fig. 2), and summarises the differences between both belts.

## STRUCTURAL DOMAINS OF THE KARAGWE-ANKOLE BELT (KAB)

Tack et al. (1994) defined an alignment of mafic and ultramafic layered igneous complexes and smaller bodies of A-type granitoid rocks, preferentially emplaced in a 10 to 35 km-wide "boundary zone" (Fig. 3), between two structurally contrasting domains in the KAB: a Western Domain (WD) and an Eastern Domain (ED).

The WD is composed of deformed, greenschist- to amphibolite-facies Mesoproterozoic metasedimentary rocks and subordinate, inter-layered metavolcanic units, intruded by numerous, extensive massifs of S-type granitoid rocks and subordinate mafic rocks (Fig. 3). In W Rwanda, preliminary data suggest that the WD is underlain by a crystalline basement of Palaeoproterozoic age (Cahen et al., 1984). Contacts between the S-type granitoid rocks and the metasedimentary rocks or crystalline basement are intrusive or tectonic with no reported unconformity.

The ED is characterised by the fading away towards the east of both deformation and metamorphism (Tack et al., 1994). Starting with a basal conglomerate, the ED unconformably overlies Archaean gneissic basement of the Tanzania craton or the Palaeoproterozoic Ruwenzori fold belt, the latter including the Buganda-Toro Supergroup (Cahen et al., 1984; Master et al., 2008; Fig. 2). In contrast to the WD, the ED is devoid of S-type granitoid rocks and of Sn-Nb-Ta-W and Au mineralisation.

The arc-shaped "boundary zone" between WD and ED, outlined by the 350 km-long alignment of the Kabanga-Musongati (KM) mafic and ultramafic layered complexes (Deblond, 1994; Tack et al., 1994; Figs. 3 and 4), marks the contact between two rheologically contrasting basement domains of the KAB: (1) lithosphere of the Palaeoproterozoic Ubende - Rusizian terranes, underlying the WD, and (2) Archaean lithosphere of the Tanzania craton, overlain unconformably by the ED sediments.

## GEOLOGICAL FRAMEWORK OF THE KARAGWE-ANKOLE BELT (KAB)

### Palaeoproterozoic basement

In the WD of Rwanda, Fernandez-Alonso and Theunissen (1998) were able to discriminate granitoid rocks, interpreted as younger intrusions, from granitic gneisses and migmatites considered as older basement rocks. Earlier studies, based on reconnaissance geochronological data or on structural and/or metamorphic characteristics observed during field mapping, had already repeatedly invoked the presence of Rusizian basement in W Rwanda, e. g. near the town of Butare (Figs. 3 and 4; Cahen et al., 1984, and references therein; Lavreau, 1985; Baudet et al., 1988; Theunissen et al., 1991).

**S-type granitoid rocks**

A large volume of two-mica granites occurs in both the KAB and KIB (Cahen et al., 1984 and references therein). Past studies of these rocks – by various authors in various countries using various methodologies (K-Ar, Rb-Sr, bulk-zircon U-Pb) – have led to confusing and/or contradictory classifications in the corresponding literature (Table 1).

In the KAB, S-type granitoid rocks occur only in the WD (Tack et al., 1994). Most past attempts at dating them used the Rb-Sr geochronometer (Burundi: Klerkx et al., 1984, 1987 – Rwanda: Gérards and Ledent, 1970; Lavreau and Liégeois, 1982 – NW Tanzania: Ikingura et al., 1990). Only Cahen et al. (1984) reported preliminary bulk-zircon U-Pb ages for granitoids in Rwanda and Burundi (Table 1).

In Burundi, Klerkx et al. (1984, 1987) linked structural observations of the granitoid rocks to their Rb-Sr ages, interpreted to reflect magma emplacement. A "Kibaran orogeny" was thus envisaged to comprise successive extensional and compressional phases, each characterised by the intrusion of syn-deformational S-type granitoids, spaced in time at c. 1330 Ma (granite 'Gr1'; type-massif: Rumeza; extensional, early-orogenic, pre-$D_1$; Fig. 5, point 2), c. 1260 Ma (granite 'Gr2'; type-massif: Mugere; extensional, syn-orogenic, syn-$D_1$; Fig. 5, point 3), and

c. 1180 Ma (granite 'Gr3'; type-massif: Kiganda; compressional, syn-orogenic, syn-$D_2$; Fig. 5, point 5). According to these authors, the protracted extensional phase $D_1$ was marked by bimodal magmatism, as indicated by the presence of gabbros in association with the Gr1-3 granitoid rocks.

The petrology of the Gr1, Gr2 and Gr3 granitoid-types points to emplacement at shallow depths of 5-10 km (Fernandez-Alonso, 1985; Fernandez-Alonso et al., 1986; Fernandez-Alonso and Theunissen, 1998). Mineralogy and whole-rock geochemistry indicate limited modal or geochemical compositional variations: syeno-monzogranites predominate with minor granodiorite and quartz-diorite. Characteristic minerals are quartz, microcline, plagioclase, muscovite and biotite in variable amounts. Accessory minerals include apatite, zircon, and sporadic rutile, garnet, tourmaline and opaques. The rocks have a calc-alkalic to slightly alkalic character and a large spread of Mg/(Mg+Fe) ratios. They are peraluminous with generally high quartz-content, and correspond to a radiometric high-K group (Fernandez-Alonso and Theunissen, 1998). Trace element geochemistry and Sr-isotopes point to a high degree of crustal contamination. Overall low REE-contents indicate only a limited differentiation trend. Based on the near-identical petrological characteristics, similar parental magmas are suggested, reflecting partial melting of a variably proportioned mixture of supracrustal metasedimentary rocks and crystalline basement rocks of presumably Palaeoproterozoic age.

The S-type granitoid rocks are systematically associated with or enclose subordinate mafic intrusive rocks. The petrological characteristics of the latter have received only limited attention in the past (Ntungicimpaye, 1984; Tack et al., 1984; Ntungicimpaye and Kampunzu, 1987, and references therein; Nzojibwami, 1987; Nahimana, 1988). They mostly form rather small bodies and pods in the granitoid rocks. The rocks are mainly coarse-grained, amphibole-bearing dolerite or gabbro. Clinopyroxene has been preserved in some gabbros that show MORB affinities (Nzojibwami, 1987). Nahimana and Tack (unpublished data) confirm the common occurrence of clinopyroxene-gabbros in part of the Gr1 Rumeza granite massif.

The S-type granitoids of the WD form extensive sill-like bodies, elongate massifs and/or domes. They are typically porphyritic and exhibit flow textures and parallel arrangements of feldspar phenocrysts that are interpreted as primary magmatic fabrics. Observed contacts with metasedimentary host rocks are either intrusive or mylonitized.

In Central and SW Burundi, the S-type granitoid bodies are sliced up by late N-S trending, E-verging, steep inverse fault zones.

**Mafic and ultramafic magmatism**

Rumvegeri (1991) and Rumvegeri et al. (2004) interpreted the “KM alignment” as remnants of an oceanic suture within the Wilson cycle-model, proposed by Kampunzu et al. (1986). However, work carried out in the framework of the UNDP mineral exploration programmes in Burundi (1970s and later), the Kabanga Nickel Project in Tanzania (Gosse, 1992; Evans et al., 1999, 2000) and PhD research in Burundi (Deblond, 1993, 1994; Tack et al., 1994; Deblond and Tack, 1999; Duchesne et al., 2004) has demonstrated unequivocally that the mafic-ultramafic intrusions of the KM alignment (Fig. 3) are Bushveld-type layered igneous complexes. They display cumulate fabrics, magmatic layering and differentiation, mantle–derived magma types, Ni-V-Ti-Fe-PGE-mineralisation and contact metamorphism aureoles in host rocks. Airborne geophysics confirm that the KM layered complexes are in continuity to the NE with a set of structurally higher emplaced mafic sills, including those located (1) north of the Kabanga massif (Evans et al., 2000) and (2) in the Bukoba Group (Fernandez-Alonso, 2007; Fernandez-Alonso et al., in prep.) of the ED (Figs. 3 and 4). The KM intrusive bodies have been emplaced under extensional regime in flat-lying sedimentary rocks in an intra-cratonic basin (Evans et al., 2000). Intrusive contacts with the metasedimentary host rocks show contact metamorphic aureoles.

The geochemical characteristics of the KM complexes are those of tholeiitic E-type MORB magmas with local crustal assimilation and tectonic setting affinities of Continental Flood Basalts (CFB). Two types of parental magma influxes have been invoked to form the various bodies of the KM alignment: a picritic batch and a more evolved batch, geochemically broadly similar in composition to the magma of the Bushveld Main Zone, both batches being derived from an enriched lithospheric mantle source (Duchesne et al., 2004). Bulk zircon U-Pb data for the Mutanga amphibole-norite of the Musongati massif (Fig. 5, point 8) returned an intercept age of 1275 ± 11 Ma (Tack et al., 1994).

In Central and SW Burundi, the KM intrusions are locally dissected by an imbricate structure of N-S trending, E-verging, steep inverse fault zones.

**A-type granitoid rocks**

In Burundi, granitoid rocks with alkaline affinities occur as a short N-S alignment of three small elongate massifs, referred to as the Gitega-Makebuko-Bukirasazi or “GMB alignment” (Tack et al., 1994; Fernandez-Alonso, 2007; Fig. 4; Fig. 5, point 10). The A-type granitoid massifs include subordinate syenites and mafic rocks, which define a geochemical differentiation trend with the granites. Parental magmas have depleted asthenospheric mantle signature (Duchesne et al., 2004). A bulk U-Pb zircon age of 1249 ± 8 Ma was obtained by Tack et al. (1994) for the Bukirasazi granite (Fig. 5, point 10), significantly older than the whole-rock Rb-Sr ages (see Table 1) of 1137 ± 39 Ma (Tack et al., 1990) and 1125 ± 25 Ma (Klerkx et al., 1987). The latter had been used by Klerkx et al. (1987) and Theunissen (1988,

1989) to constrain a phase of "late-Kibaran transpression", in which the A-type granitoid rocks represent syn-deformational (syn-$D_{2'}$) "Gr4" granites.

Contacts with the metasedimentary host rocks are either tectonic or intrusive. Where intrusive, locally developed contact metamorphic aureoles can be observed. Like the KM intrusions, the GMB rocks are affected by an imbricate structure of N-S trending, E-verging steep inverse fault zones.

**Neoproterozoic magmatism and mineralisation**

Several episodes of magmatism and/or mineralisation indicate repeated, localised reactivation of earlier structures within the KAB during the Neoproterozoic (Tack et al., 2002b; 2006). The origin and emplacement of the Neoproterozoic "tin granites" and related mineralisation(s), referred to as "post-Kibaran" by Cahen et al. (1984) and Pohl (1994), are poorly constrained. Renewed research is devoted to metallogeny and timing of emplacement of the mineralisation event(s) of this economically important metallogenic province (Dewaele et al., 2007a, b, 2008; Kokonyangi et al., 2008).

## NEW GEOCHRONOLOGICAL DATA OF THE KARAGWE-ANKOLE BELT (KAB)

We present ion microprobe SHRIMP U-Pb zircon ages for ten different rocks, all of which have previously been isotopically dated by either Rb-Sr or bulk zircon U-Pb methods (Tables 1 and 2). All mean ages in the text are quoted with 95% confidence intervals. Analytical procedures are detailed in Appendix 1. Zircon characteristics and data are listed respectively in Tables 3 and 4. We also present $^{40}Ar/^{39}Ar$ data on primary hornblende for two samples of KM layered intrusions (Musongati and Rutovu massifs). Analytical data for the samples/splits are given in Appendix 2 and individual results are listed in Table 5. Finally, laser-ablation zircon Hf data of five samples (respectively, 1 Palaeoproterozoic basement, 3 S-type granitoid rocks and 1 "tin" granite) are given. Analytical procedures are described in Appendix 3 and data are listed in Table 6. The locations of all analysed samples are shown in Fig. 5. Moreover, their "RG"-numbers of storage in the RMCA (Tervuren, Belgium) reference collections with accompanying field archives are given in Table 2**.**

**Palaeoproterozoic basement**

**Orthogneiss of the Butare area, SW Rwanda (sample Ki16)**

Sixteen analyses were conducted during a single session: they include 6 analyses of high-U rims and 10 analyses of zoned zircon (with and without rims; details in Tables 3 and 4). Nine analyses of zoned zircons are concordant to slightly discordant (< 5%) and indicate slightly dispersed $^{207}$Pb/$^{206}$Pb ages around 1980 Ma (Fig. 6a). The highly discordant position of one analysis (5c) is consistent with substantial recent Pb loss. Four $^{207}$Pb/$^{206}$Pb ratios (3, 4, 6 and 10) agree to within analytical precision and yield a weighted mean age of 1982 ± 6 Ma (MSWD = 0.82). Analyses of high-U zircon rims are near-concordant to moderately discordant and indicate a wide range of $^{207}$Pb/$^{206}$Pb ages, from 1929 to 997 Ma, consistent with variable amounts of Pb loss. The zoned zircons probably formed during igneous crystallisation of the orthogneiss protolith at about 1982 Ma. The zircon rims could be late magmatic in origin, or conceivably formed during a post-magmatic (but no younger than 1929 Ma) metamorphic event. The rims subsequently underwent at least one episode of radiogenic Pb loss, possibly during the Mesoproterozoic, probably facilitated by radiation damage due to their high U-contents.

## S-type granitoid magmatism

### Granite 'Gr1' of the Rumeza massif, Burundi (sample 63.865)

Seventeen analyses were conducted of 17 zircons (Table 3). The data range from concordant (two analyses) to strongly discordant (Fig. 6b). A strong inverse correlation (R = 0.91) between $^{206}Pb/^{238}U$ age and $^{238}U$ concentration indicates that the discordance is due to loss of radiogenic Pb. Excluding the two high-common-Pb analyses (#7, 10), the data are a good fit to a discordia and define an upper intercept age of 1383 ± 17 Ma, regarded as the crystallisation age of this Gr1 granite.

### Granite 'Gr2' of the Mugere massif, Burundi (sample Ki6684)

Twenty-four analyses were conducted of 24 crystals (Table 3). Although most analyses lie close to concordia (Fig. 6c), several are slightly normally discordant, and nine are strongly discordant. Regression of the data (excluding the most discordant analysis, #7) yields a discordia (MSWD = 0.9) with intercepts at 1382 ± 10 Ma and 321 ± 40 Ma. Because it is likely that these zircons have experienced some recent as well as ancient Pb loss, our preferred estimate of age is based on 12 analyses less than 5% discordant, which yield a weighted mean $^{207}Pb/^{206}Pb$ age of 1379 ± 10 Ma (MSWD = 0.73).

### Migmatitic paragneiss of the Mugere complex, Burundi (sample Ki21)

Twelve analyses of 12 zircons were conducted during a single session (Table 3). Slightly discordant analyses for three zircons (#1, 7, 8) indicate $^{207}Pb/^{206}Pb$ ages of 1981, 2494, and 2439 Ma. These grains are interpreted as xenocrysts, and their $^{207}Pb/^{206}Pb$ ages as minimum estimates of their crystallisation ages. The remaining nine data range from concordant to strongly discordant (Fig. 6d). The degree of discordance varies with U and Th content, implying that discordance is due to radiogenic Pb-loss, facilitated by radiation damage. Analyses #6 and 12 are 47 and 65% discordant, highly enriched in U and Th, and also have the highest corrections for common Pb. Discordia regressions, both including and excluding analyses #6 and 12, yield lower intercepts within error of 0 Ma, indicating that Pb loss in these zircons was 'geologically recent'. Excluding the two highly discordant points (#6, 12), seven analyses (inset, Fig. 6d), yield $^{207}Pb/^{206}Pb$ ratios that agree to within analytical precision and yield a weighted mean age of 1380 ± 12 Ma (MSWD = 1.43). We consider this result to represent the time of zircon crystallization.

**Granite 'Gr3' of the Kiganda massif, Burundi (sample Ki1)**

Nineteen analyses were conducted of 19 zircons (Table 3). Most crystals exhibit euhedral concentric zoning and several contain anhedral to euhedral, homogeneous (unzoned) cores. One core was sampled (described below). For all other analyses, cores were avoided. Although the majority of analyses are concordant, the dispersion of several analyses around the main group suggests that these zircons have experienced minor amounts of recent and/or ancient loss of radiogenic Pb. Five analyses are excluded from calculation of the mean age (Fig. 7a): three that are >5% normally discordant, one (#9) that has very high $^{238}U$ concentration (3720 ppm) and is strongly reversely discordant, and one (#12) that yields a highly imprecise $^{207}Pb/^{206}Pb$ age of 1287 Ma. The weighted mean $^{207}Pb/^{206}Pb$ age of 1371 ± 7 Ma (MSWD = 0.46) for the remaining 13 analyses is taken as the best estimate of the age of the Gr3 zircons. A single analysis (#5) of a large homogeneous core yielded a slightly normally discordant result with a $^{207}Pb/^{206}Pb$ age of c. 2600 Ma. The core is interpreted as a xenocryst.

**Granite of the Muramba massif, Burundi (sample Ki14)**

Nine analyses were conducted on 8 zircons during a single session (Table 3). Five analyses form a concordant group (Fig. 7b) with a weighted mean $^{207}Pb/^{206}Pb$ age of 1380 ± 6 Ma (MSWD = 0.87). The mean does not change when the two significantly discordant analyses are included, consistent with these two zircons to have undergone geologically recent Pb loss. The age of 1380 ± 6 Ma is therefore taken as the best estimate for the crystallisation of zircon in sample Ki14. The two remaining analyses (#1, 3) define near-concordant $^{207}Pb/^{206}Pb$ ages of 1460 and 1525 Ma, and presumably represent xenocrysts.

**Granite of the Kilimbi-Muzimu massif, Rwanda (sample Ki20)**

Twelve analyses were conducted on 12 zircons, including two rims, during a single session (Table 3). The data range from concordant to slightly discordant (Fig. 7c). A concordant group of 5 analyses indicates a weighted mean $^{207}Pb/^{206}Pb$ age of 1373 ± 10 Ma (MSWD = 1.26). Three analyses (#2, 4, 9) are slightly younger at about 1325 Ma, and two others (#1, 6) are about 7% discordant (#1 is also very imprecise). We consider the weighted mean age of 1373 ± 10 Ma for the concordant group of five analyses to be the best estimate of the time of zircon crystallisation, and the five younger or more discordant results to represent zircons that have undergone radiogenic Pb loss. Two rim analyses, #3 and 8, provided $^{207}Pb/^{206}Pb$ ages of 964 and 967 Ma, respectively. Their low Th/U of 0.03 is typical of metamorphic zircon, and their mean age of 966 ± 11 Ma is considered to be a reliable estimate for crystallisation of zircon rims during a metamorphic event affecting the granite.

**Mafic and ultramafic magmatism**

**Mutanga amphibole-norite of the Musongati massif, Burundi (sample DB1)**

Forty-four analyses were conducted of 44 zircons during three analytical sessions (Table 3). A similar pattern and degree of dispersion is apparent in the results from each session. Although the majority are highly dispersed and both normally and reversely discordant, there is a main group of concordant analyses at c. 1370 Ma (Fig. 7d). Apparent ages are correlated inversely with U (and Th) concentration (Fig. 8a), indicating loss of radiogenic Pb. Low-U analyses are mainly normally discordant, whereas high-U analyses tend to be reversely discordant (Fig. 8b). The high dispersion is interpreted to result from the combined effects of recent and/or ancient loss of radiogenic Pb in most zircons and enhanced sputtering of Pb relative to U due to radiation-induced microstructural changes (metamictisation) in high-U zircons (McLaren et al., 1994). The best estimate of the age of DB1 zircons is based on the group of 14 analyses that have $^{207}Pb/^{206}Pb$ ages >1350 Ma and are less than 5% discordant (Fig. 7d). These data yield a weighted mean $^{207}Pb/^{206}Pb$ age of 1374 ± 14 Ma (MSWD = 0.43), regarded as the crystallisation age of the amphibole-norite.

Two splits of primary hornblende, separated from the same amphibole-norite sample DB1, were analysed for their $^{40}Ar/^{39}Ar$ content (Table 5). The first split yielded a single release total gas age of 1372 ± 25.7 Ma, while the second split yielded a total gas age of 1380 ± 3.2 Ma (Fig. 9a). The second split showed a well-defined plateau over the final 44% of the gas with an apparent age of 1365 ± 2.1 Ma (MSWD=0.75) and a slightly older integrated age of 1378 ± 5.2 Ma (MSWD=11.2). Because of the extremely high radiogenic yield of the release steps, meaningful isochrons could not be generated. The Ca/K ratio in the hornblende is shown in Fig. 9b. There is only minor alteration of the hornblende and the preferred age for the Mutanga hornblende is taken as the plateau age of 1365 ± 2.1 Ma.

**Hornblende-granophyre of the Rutovu massif, Burundi (sample A114)**

This hornblende-granophyre (Deblond, 1993, 1994) is a local differentiate of the Rutovu massif. A total of 5 splits of primary hornblende were analyzed (Table 5). Plateau ages are defined where the total amount of gas released over three or more steps with overlapping ages is more than 40%. Total gas ages of the splits ranged from 1351 ± 3.7 Ma to 1398 ± 3.0 Ma (average 1366 Ma; Table 1; Fig. 10a-e). With the exception of split #3, the Ca/K ratios of the hornblende was fairly constant (see Fig. 10f). Split 3 also showed the clearest evidence for excess argon at high laser powers. Only two splits (Rutovu 1-88% and Rutovu-2-45%) yielded plateau ages of 1363 ± 7.4 (MSWD = 4.68) and 1386 ± 2.4 Ma (MSWD = 0.96; Fig. 10a-b). In cases where plateau criteria where not met, integrated ages were obtained over the nearly flat portion of the release spectrum. Integrated ages for splits 1-5 are as follows: Rutovu-1, 1363 ± 7.4 Ma (MSWD = 4.68; Fig. 10a); Rutovu-2, 1373 ± 4.7 Ma (MSWD=7.26; Fig. 10b); Rutovu-3, 1360 ± 3.5 Ma (MSWD=3.28; Fig. 10c); Rutovu-4, 1372

± 3.8 (MSWD=4.61; Fig. 10d) and Rutovu-5, 1350 ± 5.6 Ma (MSWD=3.27; Fig. 10e). With the exception of split #1, excess argon clearly was observed in all the release spectra to varying degrees. Fig. 11a shows a frequency histogram for apparent ages when more than 1% of the gas was released (cumulative $^{39}K$). The mean age from all steps is 1357.9 ± 19.5 Ma (95% confidence). The most radiogenic release steps are shown in Fig. 11b and these range from 1360.8 Ma (RUT-3) to 1386.2 Ma (RUT-2). The average of the most radiogenic steps is 1373.5 ± 9.6 Ma (1σ). Because of the extremely high radiogenic yield of the release steps, meaningful isochrons could not be generated. Fig. 12a-e shows plots of apparent age versus $^{37}Ca/^{39}K$ ratios for each of the Rutovu splits. Split 3 shows the largest spread in $^{37}Ca/^{39}K$ ratios suggesting some alteration of the grain (Fig. 12c). Although not shown, $^{38}Cl/^{40}Ar$ ratios also indicate only small variability with the exception of split #3. The $^{40}Ar/^{39}Ar$ age of the Rutovu hornblendes is estimated to lie between 1350.4 ± 5.6 (integrated age from split #5) and 1386 ± 2.4 Ma (plateau age from split #2). We assign an age of 1368.2 ± 17.8 Ma for the Rutovu hornblendes.

**A-type granitoid rocks**

**Granite 'Gr4' of the Bukirasazi massif, Burundi (sample LT7)**

Fifteen analyses were conducted of 15 zircons (Table 3). Most data are within error of concordia (Fig. 13a). Two analyses (#7, 11) are >5% normally discordant, indicating minor recent Pb loss, and one (#4) is more than 5% reversely discordant. The remaining data yield weighted mean $^{207}Pb/^{206}Pb$ and $^{238}U/^{206}Pb$ ages of 1205 ± 19 Ma (MSWD = 0.47) and 1207 ±

11 Ma (MSWD = 1.02). The more precise $^{238}U/^{206}Pb$ result (1205 Ma) is our preferred estimate for the age of crystallisation of this A-type granite.

**Tin-granites**

**Granite 'Gr5' of the Kasika massif, Itombwe region, DRC (sample Ki22)**

A total of eleven analyses were conducted on 11 zircons during a single session (Table 3). Concentrically zoned and homogenous, medium CL domains were analysed. Seven analyses form a near-concordant group (Fig. 13b) with a weighted mean $^{207}Pb/^{206}Pb$ age of 986 ± 10 (MSWD = 1.40). Three zircons, #4, 8, and 9, which yielded near-concordant $^{207}Pb/^{206}Pb$ ages of 1885, 2068, and 1312 Ma, respectively, are interpreted as xenocrysts. These three zircons exhibit high Th/U ratios (0.73-1.13) relative to the other zircons (0.02-0.19). We regard the $^{207}Pb/^{206}Pb$ age of 986 ± 10 Ma for the coherent, near-concordant group of seven analyses as the best estimate for the crystallisation age in sample Ki22.

**Laser-ablation zircon Hf data**

For five of the SHRIMP-dated granitoid rocks we present laser-ablation zircon Hf data. Analytical procedures are detailed in Appendix 3 and data listed in Table 6. The analysed rocks include: 1) the Rusizian basement orthogneiss of the Butare area (sample Ki16); 2) two c. 1375 Ma S-type granitoid rocks, the Muramba (Ki14) and the Kilimbi-Muzimu massifs (Ki20); 3) the c. 1375 Ma migmatitic paragneiss of the Mugere complex (Ki21) and 4) the post-Kibaran, c. 986 Ma tin-granite of Kasika (Ki22). The data show clearly that the Rusizian orthogneiss (Ki16) has a juvenile signature with $\varepsilon_{Hf}(T) \sim 0$, i.e. similar in composition to the Chondritic Uniform Reservoir (CHUR) (Fig. 14a). The $T_{DM}$ model ages, however, indicate average crustal residence times (calculated from depleted mantle values) of up to 2.4 Ga (Table 6), indicating some participation of early-Palaeoproterozoic crust in the generation of the Butare orthogneiss. The two c. 1375 Ma S-type granitoids (Ki14 and Ki20) and the migmatitic paragneiss (Ki21) show a more ancient signature with $\varepsilon_{Hf}(T)$ between -5 and -9. These negative values suggest significant participation of older crustal material in the generation of these granitoids, as would be expected from S-type granitoids which are, essentially, derived from crustal melts. $T_{DM}$ model ages are in the range 2.4-1.6 Ga, indicating a significant average crustal residence time for these rocks. The data are consistent with the derivation of the 1375 Ma suite of granitoid rocks largely through the re-melting of the c. 2.0 Ga Rusizian basement in the region.

The c. 986 Ma tin-granite (Ki22) has a very variable, but always negative $\varepsilon_{Hf}$, indicating derivation from the reworking of older crustal material, with highly variable participation of juvenile melt. $T_{DM}$ model ages are in the range 2.5-1.7 Ga, suggesting similar crustal contaminants as in the 1375 Ma granitoid suite. Overall, the Hf-isotopic data support the recurrent reworking (i.e. at c. 1375 Ma and c. 986 Ma) of the KAB's Palaeoproterozoic basement, with only limited addition of juvenile, mantle-derived components.

## DISCUSSION OF THE NEW RESULTS

### Palaeoproterozoic basement

The presence of Palaeoproterozoic basement in the WD of SW Rwanda is confirmed by the c. 1982 Ma magmatic crystallisation age of the Butare orthogneiss (sample Ki16). A c. 1929 Ma late magmatic and/or metamorphic event in the same gneiss, evidenced by two high-U zircon rim overgrowths, is in line with the timing of exhumation under amphibolite conditions of the high grade metamorphic Ubende belt (Boven et al., 1999). Note that Gérards and Ledent (1970) mention a bulk-zircon U-Pb age of 1940 ± 30 Ma, obtained on two zircon fractions of another orthogneiss sample from the Butare area (Nyamirama, sample RG 71.221).

Two zircon cores with slightly discordant $^{207}Pb/^{206}Pb$ ages of 2494 and 2439 Ma were identified in the migmatitic paragneiss of the Mugere complex (sample Ki21). They suggest derivation from either detrital successions with early-Palaeoproterozoic components or underlying early-Palaeoproterozoic basement.

One zircon core from ‘Gr3’ sample Ki1 gave an age of c. 2600 Ma. It is derived either from underlying Archaean basement or from Palaeoproterozoic basement that includes reworked detrital material derived from an Archaean source.

**S-type granitoid magmatism**

Our SHRIMP U-Pb data firmly constrain all of the analysed S-type granitoids (samples 63.865, Ki6684, Ki21, Ki1, Ki14, Ki20) in the WD of the KAB to a short time interval around a weighted mean of c. 1376 ± 5 Ma, calculated from the six new ages. This invalidates the concept of distinct melting batches and successive intrusions over a protracted period of time, on which all the existing “Kibara belt” models were founded (see our Introduction and the references therein).

## Mafic and ultramafic magmatism

The 1374 ± 14 Ma SHRIMP age of the Mutanga amphibole-norite sample (DB1) raises questions with respect to the earlier obtained 1275 Ma bulk-zircon U-Pb age (Tack et al., 1994). However, the 1374 Ma validity as emplacement age is confirmed by the $^{40}Ar/^{39}Ar$ cooling ages (see paragraph herebelow) and by the 1403 ± 14 Ma SHRIMP U-Pb age for the Kabanga North mafic-ultramafic massif (Maier et al., 2007), which can be considered similar within error limits.

Indeed, hornblende $^{40}Ar/^{39}Ar$ data from the same Mutanga sample and from the Rutovu sample (A114) suggest these intrusions cooled below the blocking temperature for hornblende at respectively c. 1365 Ma and 1368 Ma. Deblond et al. (2001) reported similar $^{40}Ar/^{39}Ar$ ages for dolerite sills and dykes, emplaced into sedimentary rocks of the Bukoba Group of the ED (Fernandez-Alonso, 2007; Fernandez-Alonso et al., in prep.; see Figs. 3, 4 and 5, and Table 2). A dolerite sill in the Kavumwe Formation (Burundi; Fig. 5, Table 2) produced cooling ages of 1360 ± 20 Ma (plagioclase) and 1340 ± 9 Ma (hornblende). A sill in the Bukoba Sandstone Formation (Tanzania; Fig. 5, Table 2) returned hornblende plateau ages of 1379 ± 10 Ma and 1355 ± 10 Ma. Incidentally, these data confirm earlier claims of a Mesoproterozoic minimum age for the Bukoba Group sedimentary succession of the ED (Tack et al., 1992; Tack, 1995). Moreover, they are in agreement with the proposed genetic link (Fig. 4) between the KM mafic and ultramafic layered intrusions and the sills of gabbro to gabbronorite composition to the E (NW Tanzania and E Burundi), which were emplaced at a higher structural level (Evans et al., 2000; Tahon et al., 2004).

Finally, palaeomagnetic data from samples of five massifs of the KM alignment (including the dated Musongati and Rutovu massifs), as well as the dated sills of the Kavumwe Formation (Figs. 4 and 5), indicate similar poles (Meert et al., 1994a, b).

An unpublished average $^{40}Ar/^{39}Ar$ plateau age of 1358 ± 13 Ma was obtained on biotite from the Kapalagulu (or Mibango) layered igneous complex (Theunissen et al., pers. comm., Fig. 2), which is located along the northern margin of the Ubende belt, less than 150 km south of the KAB. This complex intrudes the Itiaso Group (Wadsworth et al., 1982), which is exposed in a local basin (Klerkx et al., 1998). Maier et al. (2007) report a SHRIMP U-Pb zircon crystallisation age for the Kapalagulu complex of 1392 ± 26 Ma. Like the KM alignment in the boundary zone between the WD and ED of the KAB, the Kapalagulu complex was emplaced in a major crustal feature, marking the rheological boundary between two types of lithosphere: the Palaeoproterozoic Ubende shear belt and the Archaean of the Tanzania craton. Although not dated, similar petrology and mineralization documented for the Kabulyanwele complex  some 100 km SE of Kapalagulu along the Ubende trend, suggest a similar structural setting (Fig. 2; Hester et al., 1991).

The new and existing SHRIMP U-Pb and $^{40}Ar/^{39}Ar$ data constrain the KM mafic and ultramafic intrusive magmatism to the same c. 1375 Ma time frame as the S-type granitoid magmatism and associated subordinate mafic bodies, emplaced in the WD of the KAB. Together, both magmatic suites represent a prominent, coeval, bimodal magmatic event – with clear compositional gap - taking place at c. 1375 Ma.  Emplacement of the KM mantle-derived  magmatism (Fig. 4, see elliptical aeromagnetic-gravimetric thermal anomaly), originated from an enriched source, possibly old subcontinental lithospheric mantle (Tack et al., 1994; Duchesne et al., 2004). This requires opening of crustal-scale structural features, i.e. an extensional regime. Hence it did not occur during a compressional event, for which moreover there is no geological evidence at the time of emplacement. The extension mechanism itself is debatable but falls out of the scope of this paper: intra-lithosphere mantle bulging and underplating *versus* externally imposed ascent of asthenospheric plume. Anyway, we propose that underplating mantle melts, which supplied the KM magma chambers, provided the heat, necessary to trigger lower crustal melting in the WD basement and thus generate the coeval voluminous S-type granitoid melts (Henk et al., 1997). The shallow emplacement depths of the latter at or near the basement/cover interface suggest the absence of a thick lithospheric profile in the underlying Palaeoproterozoic basement, a feature to be expected for this basement under extension.

**A-type granitoid rocks**

The 1205 ± 19 Ma SHRIMP U-Pb zircon age of the Bukirasazi sample (LT7) is interpreted to represent the granitoid's emplacement age. Like with the Mutanga amphibole-norite sample (DB1), it raises questions about the earlier obtained 1249 Ma bulk-zircon age (Tack et al., 1994). Note that a granite massif in NW Burundi (Cibitoke-Kaburantwa; "CK") returned contemporaneous bulk-zircon U-Pb ages of 1210 ± 3 Ma and 1212 ± 2 Ma for respectively coarse- and fine-grained facies (Brinckmann et al., 1994, 2001), demonstrating that c. 1205 Ma magmatism in the KAB was not restricted to the GMB alignment. The petrography and mineralogy of the CK granite are very similar to those of the Bukirasazi rocks, for which a deep-seated, depleted asthenospheric mantle-derived origin was proposed (Tack et al., 1994).

Meert et al. (1994a) reported $^{40}Ar/^{39}Ar$ age determinations for the Mukanda-Buhoro massif in the KM-alignment (Fig. 4). Biotite plateau ages from 1220 ± 2 Ma to 1226 ± 4 Ma, or integrated ages of 1212 ± 4 Ma and 1214 ± 3 Ma, were obtained on drill core samples of mafic veinlets, cross-cutting the magmatic layering of the massif. Two phlogopite-calcite pairs from the same samples had previously yielded a Rb-Sr date of 1236 ± 70 Ma (Tack et al., 1990). Deblond (1995) contended that these veins are not late pegmatitic members of the Mukanda-Buhoro massif, but are related to a set of lamprophyre dykes that display co-magmatic affinities with the GMB A-type granitoids. He therefore proposed a genetic relationship with the latter, a hypothesis which the close agreement of $^{40}Ar/^{39}Ar$ dates for the mafic veinlets and the SHRIMP age for one of the GMB massifs appears to confirm.

While error limits on the earlier bulk-zircon U-Pb ages for the Mutanga and Bukirasazi samples allowed the possibility of some type of genetic link between the KM and GMB emplacement events (Tack et al., 1994), the SHRIMP data demonstrate unequivocally that emplacement of the GMB magmas in fact post-dates that of the KM complexes by c. 170 Ma.

**Tin-granites**

In contrast to earlier ages, which dated tin mineralisation rather than the emplacement of a tin granite body (Cahen et al., 1984; Pohl, 1994; Romer and Lehmann, 1995), we report a crystallisation age of 986 ± 10 Ma for the Kasika granite (Itombwe region, DRC). The emplacement appears to have been followed closely by a regional metamorphic event, as evidenced by the 966 ± 11 Ma low Th/U rim overgrowths on zircon from the Kilimbi-Muzimu S-type granite in Rwanda (sample Ki20). Unfortunately, no rims could be dated in the Kasika granite itself. However, the occurrence of two xenocrysts of Palaeoproterozoic age in the Kasika sample supports its derivation through partial melting of much older crustal material, in line with the Hf data that suggest a variable, but significant crustal component in the Kasika granite.

## RECENT DATA FOR THE KIBARA BELT (KIB)

The most recent field mapping and laboratory work in the Kibara belt (KIB) has been carried out in the Mitwaba square degree sheet (SDS), which includes the Kibara Mountains type area (Fig. 1a; Kokonyangi, 2001; Kokonyangi et al., 2001a, b, 2002, 2004a, b, 2005, 2006). The general setup is similar to the KAB with S-type granitoid rocks and minor associated mafic rocks (metagabbro and amphibolite) intruding supracrustal metasedimentary rocks. SHRIMP U-Pb zircon age determination on five samples of the Mitwaba granitoid rocks show that they were emplaced over a short period of time around the mean of 1381 ± 8 Ma (Kokonyangi et al., 2004a). Geochemical data suggest that the granitoid rocks have almost similar compositions, but were derived from different sources through similar petrogenetic processes. TIMS U-Pb single zircon igneous crystallisation ages on two samples of mafic-intermediate complexes associated with the granitoid rocks show that the former are coeval (c. 1.39-1.38 Ga; errors not given) with the granitoid rocks (Kokonyangi et al., 2005).

One of the inherited zircon cores of the studied granitoid rocks returned a U-Pb age of 1929 ± 21 Ma, alluding to the presence of Palaeoproterozoic basement, although inheritance from a younger detrital source cannot be ruled out.

Three SHRIMP measurements on metamorphic zircon overgrowths gave an age of 1079 ± 14 Ma, which has been interpreted as dating the main tectono-metamorphic event that shaped the morpho-structural trend of the KIB (Kokonyangi et al., 2004a). If confirmed elsewhere in the KIB, this would mean that compressional deformation (or at least one such event) post-dates the coeval bimodal magmatic event by about 300 Ma, shifting this compressional event to the time frame of the Southern Irumide collision (Johnson et al., 2006).

Tin and columbite-tantalite (coltan) mineralisation, such as reported in the KAB, also occurs in the Mitwaba SDS.

## TECTONIC SETTING OF THE 1375 MA MAGMATIC EVENT

In the KAB voluminous emplacement of the coeval 1375 Ma bimodal magmatism has been ascribed to extension. During ascent the mantle-derived magmas have taken advantage of the regionally occurring zone of weakness in the lithosphere, i.e. the rheological boundary between the Archaean craton of Tanzania, to the east, and the adjacent Palaeoproterozoic basement (2.1 Ga mobile belt), to the west. Moreover, the mantle-derived magmas initiated concomittantly large-scale, crustal melting preferentially of the Palaeoproterozoic basement under extension and characterized by the absence of a thick lithospheric profile in contrast to the nearby Archaean craton. Such petrogenetic processes have intra-plate characteristics and are thus not associated with normal plate boundary processes nor with their typical magmatism. On the contrary, they may include rift-related packages, characteristically associated with successful or attempted, though unsuccessful, continental break-up as was the case here.

Intra-plate characteristics of the KAB are further evidenced by the proven occurrence of Palaeoproterozoic basement (this paper) as well as by the lack of remnant oceanic crust, ophiolites or juvenile volcanic arc type magmatic rocks.

In the KIB, a continental margin arc setting has been suggested for the mafic-intermediate igneous rocks of the Mitwaba SDS based on the geochemistry of these rocks (Kokonyangi et al., 2004a, 2005; 2006), implying the subduction of oceanic lithosphere until c. 1.38 Ga. However, this compressional model is hampered by the absence of ophiolite remnants and deep marine deposits. On the contrary, the metasedimentary successions of the Mitwaba SDS record shallow-water, terrigenous deposition, more in keeping with an intra-cratonic basin or shallow marine, proximal conditions. Geochemical characteristics of the Mitwaba S-type granitoid rocks show strong similarities with highly peraluminous granitoid rocks of the Hercynian and Lachlan Fold Belts, the latter being known to result from significant heating at time of extension (Collins, 1996).

Felsic components of bimodal magmatism can display quite variable isotopic and trace element characteristics, because such felsic magmas are derived from partial melting of lower crust. Therefore, these magmas will inherit some of the geochemical characteristics of the protolith (Bryan et al., 2002). Their parameters can therefore not be regarded as unique identifiers of the setting and origin of the magmatism. Geochemical characteristics of S-type granitoids, extracted from e.g. a protolith with strong juvenile patterns, will reflect first of all their source(s) of derivation and the melting and crystallisation history of the protolith melts. Thus, they cannot be used in a straightforward manner to assess the tectonic regime under which the granitoid rocks were formed.

Finally, the S-type granitoids of both the KAB and the KIB show no temporal nor spatial zonation. Hence no simple genetic relationship may be established between different granitoid types and successive collisional geodynamic environments.

It must be observed that Kokonyangi's extensive recent work in the KIB is in line with Kampunzu et al. (1986), Rumvegeri (1991) and Rumvegeri et al. (2004), who viewed the "Kibaran orogeny" in a subduction-collision setting, based essentially on geochemical grounds. Kampunzu (2001) and Kokonyangi et al. (2007) even envisaged a continuous 3000-km long "Kibaran orogenic system", encompassing several Mesoproterozoic segments of a belt, wrapped around the southern African Kaapvaal craton and throughout the Central African Congo-Tanzania-Bangweulu cratonic blocks. Based on recent single-zircon geochronological data, De Waele et al. (2003) indicated that a direct correlation between

Mesoproterozoic terrains among both cratonic blocks appears unlikely (see also De Waele et al., 2009 and references therein).

Finally, it is worth noting that – apart from the bimodal magmatic rocks in the KAB and the KIB - another large coeval bimodal magmatic unit, i.e. the Cunene Anorthosite Complex of SW Angola, was emplaced at the SW margin of the Congo craton at the same time (Mayer et al., 2004; Drüppel et al., 2007 and references therein). The Cunene Complex lies some 1200 km to the SW of the KIB and about 2100 km from the KAB.

## THE NEED FOR REDEFINING THE TERM "KIBARAN"

For decades, the term "Kibaran" has been used to identify or describe the "orogenic cycle" occurring in Central Africa in Mesoproterozoic times (1.4-1.0 Ga; Cahen et al., 1984 and references therein). Based on radiometric ages of S-type granitoid magmatism and regional geological data, this "Kibaran orogenic cycle" was considered to have a protracted character with a "culmination from before 1370 Ma to 1310 Ma" (Cahen et al., 1984, page 194), followed by late-Mesoproterozoic phases. The Neoproterozoic "tin granites" and related mineralisation(s) of c. 970 Ma were referred to as "post-Kibaran" by Cahen et al. (1984) and Pohl (1994).

The term "Kibaran" was subsequently exported to other parts of Africa to denote any orogenic event, shown by radiometric dating to fall within the same prolonged time span. Such chronostratigraphic (mis)use of the term has introduced a lot of semantic confusion and debate among geoscientists working in Africa. In more recent times, the term has even become linked to the global chain of c. 1.0 Ga collisional events ("Grenvillian"), leading to the amalgamation of the Rodinia supercontinent (Tack et al., 1995, 2002a, 2002b, 2006, 2008; Kampunzu, 2001; Kokonyangi et al., 2006; De Waele et al., 2006; McCourt et al., 2006; Eglington, 2006; Becker et al., 2006; Hanson et al., 2006; Li et al., 2008).

The single-zircon U-Pb data, presented in this paper and in Kokonyangi et al. (2004a; 2005), demonstrate that the coeval bimodal magmatism in both the KAB and the KIB took place in a very short time span around 1375 Ma.

In view of the preceding, the hitherto-adopted concept of a “Kibaran” orogeny or orogenic cycle, affecting the KAB and the KIB contemporaneously over a prolonged time span during the second half of the Mesoproterozoic, can no longer be maintained. We therefore propose to restrict the future use of the term “Kibaran” to the c. 1375 Ma “tectono-magmatic event”, corresponding to the prominent emplacement of the bimodal magmatism under intra-cratonic regional-scale extensional stress regime as described herein.

Based on the intra-cratonic (intra-plate) nature of the KAB and the KIB, it can be argued that post- “Kibaran event” compressional deformation, including folding and thrusting within both belts, must reflect far-field effects of global orogenic events, external to the craton. Results in progress on this topic will be addressed in the forthcoming companion paper (Fernandez-Alonso et al., 2009; in prep.).

## CONCLUSIONS

The peculiar structural setting of the redefined (this paper) “Karagwe-Ankole belt” (KAB) and of the “Kibara belt” (KIB), separated by Palaeoproterozoic terranes (Ubende belt – Rusizian basement), is fundamental to the understanding of the geodynamic, magmatic and mineralisation history of both redefined Mesoproterozoic belts. The new age data for the KAB and the KIB completely modify the timing and duration of the “Kibaran orogeny”. In the light of new SHRIMP U-Pb zircon, $^{40}Ar/^{39}Ar$ and laser-ablation zircon Hf data, the multi-phase Rb-Sr based time frame, on which previous geodynamic interpretations of both belts had been based in the last decades, has to be discarded.

The c. 1982 Ma magmatic crystallisation age of the Butare orthogneiss protolith indicates that, at least in SW Rwanda, Palaeoproterozoic basement is exposed within the WD of the KAB. Moreover, the presence of xenocrystic components of Palaeoproterozoic age in later felsic magmatic rocks supports the idea that most, if not all of the WD, and possibly of the KIB is underlain by Palaeoproterozoic basement.

The c. 1375 Ma unequivocally dated coeval bimodal magmatic event in the KAB, documented in the bulk of our paper, is indicative of intra-cratonic regional-scale emplacement under extensional stress regime. During ascent the mantle-derived magmas originating from an enriched lithospheric source have taken advantage of the regionally occurring crustal-scale zone of weakness in the KAB, i.e. the rheological boundary between the Archaean craton of Tanzania, to the east, and the adjacent Palaeoproterozoic basement (2.1 Ga mobile belt), to the west, both overlain by Mesoproterozoic (meta)sedimentary rocks.

Moreover, the mantle-derived magmas initiated concomittantly large-scale, crustal melting preferentially of the Palaeoproterozoic basement under extension and characterized by the absence of a thick lithospheric profile in contrast to the nearby Archaean craton.

The short-lived but prominent c. 1375 Ma “tectono-magmatic event” has intraplate characteristics, is rift-related and indicative of attempted, though unsuccessful continental breakup in the case of both the KAB and the KIB. In future, the use of the term “Kibaran” should be restricted only to this “tectono-magmatic event”. Following this “Kibaran event”, A-type granitoid rocks have been emplaced very locally in the WD of the KAB at c. 1205

Ma, followed by tin granites - one intruded at c. 986 Ma - which gave rise to the world-class Sn-metallogenic province overprinting large areas of both the KAB and the KIB.

The range of magmatic suites reported for the KAB, together with recent data on granitoid and mafic-intermediate rocks of the Mitwaba SQS in the KIB, make it unlikely that significant magmatic suites have been overlooked. Remarkable similarities exist thus between the two belts, especially for the timing of emplacement of 1) the S-type granitoid rocks and associated subordinate mafic-intermediate igneous rocks (bimodal magmatism) and 2) the tin mineralisations. Note, however, that no mafic and ultramafic layered complexes, nor A-type granitoid rocks have been identified up to now in the KIB.

Compressional deformation reflecting far-field effects of global orogenic events, external to the craton, post-dates the c. 1375 Ma "Kibaran event" and is consistent with the proposed time-frame for Rodinia amalgamation at c. 1.0 Ga.

**ACKNOWLEDGMENTS**

The late Professor Chris Mc. Powell is thanked to have introduced L. Tack to the Tectonics Special Research Centre (TSRC) staff and facilities. Authors M. Wingate and B. De Waele were attached to the TSRC at the time and gratefully acknowledge its support. U-Pb measurements were conducted using the Perth SHRIMP II ion microprobes at the John de Laeter Centre for Mass Spectrometry at Curtin University of Technology, in Perth, Australia. Hf data were obtained at the Laser Ablation facilities of the ARC National Key Centre for Geochemical Evolution and Metallogeny of Continents (GEMOC) at Macquarie University, Sydney. This is a (very late) contribution to the International Geological Correlation Programme (IGCP) Projects 418 and 440.

The authors thank P. Cawood, S. McCourt and J. Jacobs for their thorough review of the submitted manuscript. Their comments and suggestions have substantially improved the first draft of this paper.

## FIGURE CAPTIONS

Figure 1a: Sketch map of the two distinct "Karagwe-Ankole belt" (KAB) and the "Kibara belt" (KIB), as redefined in this paper (modified after Cahen and Snelling, 1966 and including various earlier names, see text). Note the general predominant NE-SW trend of both belts, clearly interrupted by the NW-SE trending Ubende belt-Rusizian basement high; "Ki Mt": Kibara Mountains type locality; "M" = Mitwaba town; Elisabethville = Lubumbashi town; box cutting the KAB and KIB: region covered by Fig. 1b; box after Brinckmann et al., 2001: general sketch map of the Kibaran belt, often – wrongly – represented as one single and continuous belt (see also Cahen et al., 1984).

Figure 1b: Synthetic Aperture Radar (SAR) mosaic image of the box area in Fig. 1a showing the prominent structural and physiographic break in continuity between the KAB and the KIB, marked by the Ubende belt-Rusizian basement.

Figure 2 (colour): Regional setting of the Karagwe-Ankole belt (KAB) in its Proterozoic and Archaean framework (in Fernandez-Alonso, 2007 after CGMW, 1986-1990; compare also with Fig. 1a, box after Brinckmann et al., 2001); note the NW-SE trending Ubende belt-Rusizian basement high marking the SW limit of the KAB and showing a break in continuity between the KAB and the Kibara belt (KIB). The region in green, north of the Rusizian basement (blue colour) and west of the Western Rift, is obtained from (successive) map compilations that lack new field data for more than fifty years. Its extent is probably (largely) overestimated. In this paper (see text), it is left undefined for now, and its complex relationship to the KAB is not a topic of the present article. Lakes are named after their initial: A: Albert; E: Edward; V: Victoria; K: Kivu; T: Tanganyika; M: Mweru and B: Bangweulu; Ka and Kab: respectively Kapalagulu and Kabulyanwele layered igneous complexes; Ru. b.: Palaeoproterozoic Ruwenzori fold belt (see explanations in text).

Figure 3 (colour): Sketch map of the Karagwe-Ankole belt (KAB) and regional framework (slightly modified after Tack et al., 1994; Fernandez-Alonso, 2007); note structural domains within the KAB: WD (Western Domain) separated from the ED (Eastern Domain) by a boundary zone, comprising the Kabanga-Musongati (KM) alignment of mafic and ultramafic layered complexes; K: Kabanga massif; M: Musongati massif; B: Butare town.

Figure 4 (colour): Contrast-enhanced Total Magnetic Intensity (TMI) map of the Kabanga-Musongati alignment (data from the aeromagnetic compilation by African Magnetic Mapping Project). WD: Western Domain; BZ: Boundary Zone (as defined by TMI), overlapping broadly with the "boundary zone" in Fig. 3 (see also Tack et al., 1994); ED: Eastern Domain; But: Butare town (and exposed Palaeoproterozoic block);

*Green:* mafic/ultramafic layered complexes of the KM-alignment with names of the five complexes north of Kabanga (serial number: 1-5: after Evans et al. (2000): - 1: Burigi – 2: Ruiza – 3: Kibamba – 4: Kanyautenge – 5: Luhuma – 6: Kabanga – 7: Mulemera – 8: Nyabikere – 9: Waga – 10: Mukanda-Buhoro-Musongati – 11: Rutovu – 12: Nkoma "hidden" body (not outcropping; further explanations of regional setting in Tack et al., 1992);

*Blue*: region covered by gabbro-noritic sills intrusive in the Bukoba Group (Fernandez-Alonso, 2007; Fernandez-Alonso et al., in prep); : B and K refer to the tabular siliciclastic rocks of the Bukoba Group, respectively the former "Bukoba Sandstone"- and "Kavumwe" lithostratigraphic units, now ranked as Formations (Fernandez-Alonso, 2007); $^{40}Ar/^{39}Ar$ emplacement ages of sills are from Deblond et al. (2001); see also Table 2 and Fig. 5;
*Reddish-Pink*: region of elongated bodies of Gitega-Makebuko-Bukirasazi (GMB) A-type granitoid rocks;
*Dashed black line*: Outline of elliptical aeromagnetic structure, coinciding with gravimetric structure;
*Brown reddish dots*: enhancement of contact between BZ and WD, marking the indentor palaeomorphology of the Archaean Tanzania craton (see also Figs. 3 and 5), with indentor angle at northern tip of massif 9 (Waga); note that the gravimetric structure outlined by dashed black line coincides with the indentor palaeomorphology;
*Yellow*: region covered by younger Kabuye-Gagwe (K-G) amygdaloidal basalts: c. 795 Ma Continental Flood Basalts (CFB) of the Neoproterozoic Malagarazi-Nyamuri (formerly, Bukoba) Supergroup (further explanations of regional setting in Deblond et al., 2001);
*Solid black lines*: Faults.
Note that in the WD, the mafic rocks, which are omnipresent within the S-type granitoid rocks (see explanation in text) although in subordinate volumes, and which also may intrude as small bodies into the metasediments, are not indicated on this map.

Figure 5 (colour): GIS-based "Geological Map of the Mesoproterozoic Karagwe-Ankole belt (KAB) of Fernandez-Alonso (2007), encompassing a surface of c. 7 square degrees; superposed: localisation of geochronology samples discussed in text: 1: Orthogneiss of the Butare area, SW Rwanda (sample Ki16; SHRIMP); 2: Granite "Gr1" of the Rumeza massif, Burundi (sample 63.865; SHRIMP); 3: Granite "Gr2" of the Mugere massif, Burundi (sample Ki6684; SHRIMP); 4: Migmatitic paragneiss of the Mugere complex, Burundi (sample Ki21; SHRIMP); 5: Granite "Gr3" of the Kiganda massif, Burundi (sample Ki1; SHRIMP); 6: Granite of the Muramba massif, Burundi (sample Ki14; SHRIMP); 7: Granite of the Kilimbi-Muzimu massif, Rwanda (sample Ki20; SHRIMP); 8: Mutanga amphibole norite of the Musongati massif, Burundi (sample DB1; SHRIMP and $^{40}Ar/^{39}Ar$); 9: Hornblende granophyre of the Rutovu massif, Burundi (sample A114; $^{40}Ar/^{39}Ar$); 10: Granite "Gr4" of the Bukirasazi massif, Burundi (sample LT7; SHRIMP); 11: Granite "Gr5" of the Kasika massif (Itombwe region), DRC (sample Ki22; SHRIMP); 12: dolerite sill in the Bukoba Group (Fernandez-Alonso, 2007; Fernandez-Alonso et al., in prep), formerly "Kavumwe" lithostratigraphic unit, $^{40}Ar/^{39}Ar$ ages in Deblond et al. (2001); 13: dolerite sill in the Bukoba Group (Fernandez-Alonso, 2007; Fernandez-Alonso et al., in prep), formerly "Bukoba Sandstone" lithostratigraphic unit, $^{40}Ar/^{39}Ar$ ages in Deblond et al. (2001); compare also with data in Tables 1 and 2.

Figure 6: U-Pb analytical data for zircons from (a) Butare orthogneiss sample Ki16, (b) Rumeza granite sample 63.865, (c) Mugere granite sample Ki6684, and (d) Mugere migmatitic paragneiss sample Ki21. The preferred age for each sample is shown with 95% confidence limits. In each case, analyses not included in calculating the preferred age are shown with filled squares; analyses of xenocrystic zircons are shown with diamond symbols. In (b), the IDTIMS result of Ledent (1979) is shown.

Figure 7: U-Pb analytical data for zircons from (a) Kiganda granite sample Ki1, (b) Muramba granite sample Ki14, (c) Kilimbi-Muzimu granite sample Ki20, and (d) Mutanga amphibole norite sample DB1. The preferred age for each sample is shown with 95% confidence limits. In each case, analyses not included in calculating the preferred age are shown with filled squares; analyses of xenocrystic zircons are shown with diamond symbols. In (d), the IDTIMS results of Tack et al. (1994) are shown.

Figure 8: (a) Variation of $^{207}Pb/^{206}Pb$ age with $^{238}U$ concentration in zircons from Mutanga amphibole norite sample DB1. The equation of the best-fit regression line is shown; R, Pearson's correlation coefficient. Error bars are 1$\sigma$; (b) Degree of discordance ([1-$^{206}Pb/^{238}U$ age / $^{207}Pb/^{206}Pb$ age] x 100) versus $^{238}U$ concentration.

Figure 9: (a) Musongati sample: stepwise gas release plot for split #1 and single release age data for splits #1 and 2 (b) $^{37}Ca/^{39}K$ stepwise release plot for Musongati split #1.

Figure 10: (a) Stepwise gas release plot for Rutovu split #1; (b) Stepwise gas release plot for Rutovu split #2; (c) Stepwise gas release plot for Rutovu split #3; (d) Stepwise gas release plot for Rutovu split #4; (e) Stepwise gas release plot for Rutovu split #5; (f) $^{37}Ca/^{39}K$ stepwise release plot for each of the splits (colour coded).

Figure 11: (a) Frequency histogram of apparent ages for the Rutovu splits 1-5 where cumulative argon release in each step was 1% or more. (b) Apparent ages of the most radiogenic gas fraction from each of the Rutovu splits.

Figure 12: (a) Plot of $^{37}Ca/^{39}K$ versus apparent age for each release of split #1. (b) Plot of $^{37}Ca/^{39}K$ versus apparent age for each release of split #2. (c) Plot of $^{37}Ca/^{39}K$ versus apparent age for each release of split #3 (d) Plot of $^{37}Ca/^{39}K$ versus apparent age for each release of split #4 and (e) Plot of $^{37}Ca/^{39}K$ versus apparent age for each release of split #5.

Figure 13: U-Pb analytical data for zircons from (a) Bukirasazi granite sample LT7, and (b) Kasika granite sample Ki22. The preferred age for each sample is shown with 95% confidence limits. In each case, analyses not included in calculating the preferred age are shown with filled squares; analyses of xenocrystic zircons are shown with diamond symbols. A single highly discordant analysis is not shown. In (a), the IDTIMS results of Tack et al. (1994) are shown.

Figure 14: (a) $\varepsilon_{Hf}$ versus emplacement age plot for samples from the KAB; (b) $Hf_i$ versus emplacement age plot for samples from the KAB.

## TABLE CAPTIONS

Table 1: Comparison of the three emplacement ages for intrusive rocks in the KAB (first column) obtained by SHRIMP and $^{40}Ar/^{39}Ar$ dating (this paper: see respectively, c. 1375 Ma, c. 1205 Ma and c. 986 Ma) with earlier scattered "Kibaran ages", obtained by various authors at various times and in various countries by Rb-Sr method or bulk zircon (= italic figures; asterisk refers to a Burundi sample); note that all earlier "ages" converge to the three emplacement ages obtained in this paper; also note the confusing terminologies for the "Kibaran" granitoids of: 1) Katanga (DRC): A, B, C, D and E-types; 2) Rwanda : G1, G2, G3 and G4-types; and 3) Burundi: Gr1, Gr2, Gr3, Gr4 and Gr5-types; see in particular the distinct "G" and "Gr" terminologies (and apparent "ages") between adjacent Rwanda and Burundi. Finally, note also the three following bulk zircon ages (Cahen et al., 1984, page 191) for a "Kibaran" granite (including already the "oldest" age of 1370 Ma ! ): 1) two discordant zircon fractions from a granitoid near Gitarama (Rwanda) yielded Concordia intercept ages of 1348 and 63 Ma (reported without uncertainties); 2) four zircon fractions from a granitoid rock near Gatsibo (Rwanda) defined intercept ages of 1317 ± 67 and -358 ± 440 Ma and a mean $^{207}Pb/^{206}Pb$ age (i.e. assuming zero-age Pb loss) of 1362 Ma; 3) two zircon fractions of the Nyamurungu granite in Burundi defined intercept ages of 1370 and 14 Ma; the latter are "recalculated" ages (after Ledent, 1979), as a result of change in value of adopted decay constants. The Nyamurungu granite forms part of the Gr1 type Rumeza granite massif (Fig. 5, point 2), as defined by Klerkx et al. (1984, 1987).

Recent ages of Kokonyangi (2004a, 2006) for the KIB are omitted as they match our own c. 1375 Ma ages in the KAB. See also Fig. 5 for localisation of analysed samples (this paper).

Table 2 : Overview of analysed samples with new isotopic ages (this paper: serial numbers 1 to 11; see Fig. 5 for localisation) and of two $^{40}Ar/^{39}Ar$ ages in Deblond et al. (2001, serial numbers 12-13, see Fig. 5); locality names, comparison to previous classification(s) and "age" data in bibliographic references: (1): (Deblond et al., 2001); (2) (Cahen et al., 1984); (3) (Briden et al., 1971); (4) (Klerkx et al., 1984);(5) (Tack et al., 1994); (6) (Tack et al., 1990); (7) (Cahen and Ledent, 1979); (8) (Ikingura et al., 1990); (9) (Lavreau and Liégeois, 1982); (10) (Ledent, 1979);
New ages are SHRIMP zircon $^{207}Pb/^{206}Pb$ ages, except where (*) indicates $^{40}Ar/^{39}Ar$ age (all ages reported with 95 % confidence limits);
Last column: list of RG-numbers referring to RMCA (Tervuren, Belgium) sample collection and archives.

Table 3: Characteristics of analysed zircons

Table 4: Ion microprobe U-Pb (SHRIMP) data of analysed zircons

Table 5: $^{40}Ar/^{39}Ar$ data of primary hornblende of Rutovu and Musongati massifs

Table 6: Zircon LAM-ICP-MS Lu/Hf data

## BIBLIOGRAPHIC REFERENCES


Alexander, E.C. Jr., Michelson, G.M., and Lanphere, M.A., 1978. A new $^{40}Ar/^{39}Ar$ dating standard, *in* Zartman, R.E., ed., Short papers of the 4th International Conference on Geochronology, Cosmochronology, Isotope Geology: U.S. Geol. Survey Open-File Rept. 78-701, 6-8.

Baudet, D., Hanon, M., Lemonne, E. and Theunissen, K., 1988. Lithostratigraphie du domaine sédimentaire de la chaine Kibarienne au Rwanda. Annales de la Société Géologique Belge, 112, 225-246.

Becker, T., Schreiber, U., Kampunzu, A. and Armstrong, R., 2006. Mesoproterozoic rocks of Namibia and their plate tectonic setting. Journal of African Earth Sciences, 46, 112-140.

Blichert-Toft, J., Chauvel, C. and Albarede, F., 1997. The Lu-Hf geochemistry of chondrites and the evolution of the mantle-crust system. Earth and Planetary Science Letters, 148, 243-258.

Boven, A., Theunissen, K., Sklyarov, E., Klerkx, J., Melnikov, A., Mruma, A. and Punzalan, L., 1999. Timing of exhumation of a high-pressure granulite terrane of the Palaeoproterozoic Ubende belt (west Tanzania). Precambrian Research, 93, 119-137.

Briden, J.C., Piper, J.D., Henthorn, D.I., Rex, D.C., 1971. New paleomagnetic results from Africa and related potassium-argon age determinations. 15th Annual Report, Research Institute African Geology, University of Leeds, 46-50.

Brinckmann, J., Lehmann, B., Hein, U., Höhndorf, A., Mussallam, K., Weiser, T. and Timm, F., 2001. La géologie et la minéralisation primaire de l'or de la chaîne Kibarienne, nord-ouest du Burundi, Afrique orientale. Geologische Jahrbuch Reihe, D 101: 3-195.

Brinckmann, J., Lehmann, B. and Timm, F., 1994. Proterozoic gold mineralization in NW Burundi. Ore Geology Reviews, 9, 85-103.

Bryan, S.E., Riley, T.R., Jerram, D.A., Leat, P.T., and Stephens, C.J., 2002. Silicic volcanism: an under-valued component of large igneous provinces and volcanic rifted margins. i*n*: Menzies, M.A., Klemperer, S.L., Ebinger, C.J., Baker, J. (eds.), Magmatic Rifted Margins. Geological Society of America Special Paper, 362, 99-118.

Buchwaldt, R., Toulkeridis, T., Todt, W. and Ucakuwun, E.K., 2008. Crustal age domains in the Kibaran belt of SW-Uganda: Combined zircon geochronology and Sm–Nd isotopic investigation Journal of Africal Earth Sciences, 51, 4-20.

Cahen, L. and Snelling, N.J., 1966. The geochronology of Equatorial Africa, North-Holland Publishing Company, Amsterdam, 195 pp.

Cahen, L. et Ledent, D., 1979. Précisions sur l'âge, la pétrogenèse et la position stratigraphique des "granites à étain" de l'est de l'Afrique Centrale. Bulletin Société belge Géologie, 88, 33-49.

Cahen, L., Snelling, N.J., Delhal, J., Vail, J.R., Bonhomme, M. and Ledent, D., 1984. The geochronology and evolution of Afric. Oxford University Press, Oxford, 512 pp.

Claoué-Long, J., Compston, W., Roberts, J. and Fanning, C.M., 1995. Two Carboniferous ages: a comparison of SHRIMP zircon dating with conventional zircon ages and $^{40}Ar/^{39}Ar$ analysis. In: W.A. Berggren, D.V. Kent, M.-P. Aubry and J. Hardenbol (Editors), Geochronology, time scales and global stratigraphic correlation. SEPM (Society of Sedimentary Petrology) Special Publication, pp. 3-21.

Collins, W.J., 1996. Lachlan Fold Belt granitoids: products of three-component mixing. Geological Society America Special Papers, 315, 171-178.

Compston, W., Williams, I.S. and Meyer, C., 1984. U-Pb geochronology of zircons from lunar breccia 73217 using a sensitive high mass-resolution ion microprobe. Journal of Geophysical Research, 89, 525-534.

De Waele, B., Wingate, M.T.D., Mapani, B. and Fitzsimons, I.C.W., 2003. Untying the Kibaran knot: A reassessment of Mesoproterozoic correlations in southern Africa based on SHRIMP U-Pb data from the Irumide belt. Geology, 31, 509-512.

De Waele, Kampunzu, A.B., Mapani, B. and Tembo, F., 2006. The Mesoproterozoic Irumide belt of Zambia. Journal of African Earth Sciences, 46, 36-70.

De Waele, B., Fitzsimons, I.C.W., Wingate, M.T.D., Tembo, F., Mapani, B. and Belousova, E.A., 2009. The geochronological framework of the Irumide Belt: A prolonged crustal history along the margin of the Bangweulu Craton. American Journal of Science, 309, 132-187.

Deblond, A., 1993. Géologie et pétrologie des massifs basiques et ultrabasiques de la ceinture Kabanga-Musongati au Burundi. PhD Thesis (unpublished), Université de Liège (Belgium), 235 pp.

Deblond, A., 1994. Géologie et pétrologie des massifs basiques et ultrabasiques de la ceinture Kabanga-Musongati au Burundi. Annales du Musée Royal de l'Afrique Centrale, Tervuren (Belgique), Sciences géologiques, 99, 1-123.

Deblond, A., 1995. Lamprophyres of Burundi: a review. Royal Museum for Central Africa, Tervuren (Belgium), Dépt. Géologie Minéralogie, Ann. Rep. 1993-1994, 91-97.

Deblond, A. and Tack, L., 1999. Main characteristics and review of mineral resources of the Kabanga-Musongati mafic-ultramafic alignment in Burundi. Journal of African Earth Sciences, 29, 313-328.

Deblond, A., Punzalan, L.E., Boven, A. and Tack, L., 2001. The Malagarazi Supergroup of SE Burundi and its correlative Bukoban Supergroup of NW Tanzania: Neo - and Mesoproterozoic chronostratigraphic constraints from Ar-Ar ages on mafic intrusive rocks. Journal of African Earth Sciences, 32, 435-449.

Dewaele, S., Tack, L., Fernandez-Alonso, M., Boyce, A. and Muchez, P., 2007a. Cassiterite and columbite-tantalite mineralisation in pegmatites of the northern part of the Kibara orogen (Central Africa): the Gatumba area (Rwanda), 9th Biennal SGA meeting. Mineral exploration and research: digging deeper, Dublin, Ireland, pp. 1489-1492.

Dewaele, S., Tack, L., Fernandez-Alonso, M., Boyce, A. and Muchez, P., 2007b. Cassiterite mineralization in vein-type deposits of the Kibara orogen (Central Africa): Nyamiumba (Rutongo area, Rwanda). 9th Biennal SGA meeting. Mineral exploration and research: digging deeper, Dublin, Ireland, pp. 1007-1010.

Dewaele, S., Tack, L. and Fernandez, A.M., 2008. Cassiterite and columbite-tantalite (coltan) mineralization in the Mesoproterozoic rocks of the northern part of the Kibara orogen (Central Africa): preliminary results. Bulletin des Séances de l’Académie royale des Sciences d’Outre-Mer / Mededelingen der Zittingen van de Koninklijke Academie voor Overzeese Wetenschappen, Brussels, 54, 3, 341-357.

Drüppel, K., Littmann, S., Romer, R.L. and Okrusch, M., 2007. Petrology and isotope geochemistry of the Mesoproterozoic anorthosite and related rocks of the Kunene Intrusive Complex, NW Namibia. Precambrian Research, 156, 1-31.

Duchesne, J.C., Liégeois, J.P., Deblond, A. and Tack, L., 2004. Petrogenesis of the Kabanga-Musongati layered mafic-ultramafic intrusions in Burundi (Kibaran Belt): geochemical, Sr-Nd isotopic constraints and Cr-Ni behaviour. Journal of African Earth Sciences, 39, 133-145.

Eglington, B., 2006. Evolution of the Namaqua-Natal Belt, southern Africa – A geochronological and isotope geochemical review. Journal of African Earth Sciences, 46, 93-111.

Evans, D.M., Byemelwa, L. and Gilligan, J., 1999. Variability of magmatic sulphide compositions at the Kabanga nickel prospect, Tanzania. Journal of African Earth Sciences, 29, 329-351.

Evans, D.M., Boadi, I., Byemelwa, L., Gilligan, J., Kabete, J. and Marcet, P., 2000. Kabanga magmatic sulphide deposits, Tanzania: morphology and geochemistry of associated intrusions. Journal of African Earth Sciences, 30, 651-674.

Fernandez-Alonso, M., 1985. Bijdrage tot de geologische en petrologische kennis van granietische gesteenten uit het Burundiaan van Burundi. PhD Thesis (unpublished), University of Ghent (Belgium), 313 pp.

Fernandez-Alonso, M., 2007. Geological Map of the Mesoproterozoic Northeastern Kibara Belt. Royal Museum for Central Africa, Tervuren (Belgium): catalogue of maps and digital data, and "http://www.africamuseum.be"

Fernandez-Alonso, M. and Theunissen, K., 1998. Airborne geophysics and geochemistry provide new insights in the intracontinental evolution of the Mesoproterozoic Kibaran belt (Central Africa). Geological Magazine, 135, 203-216.

Fernandez-Alonso, M., Lavreau, J. and Klerkx, J., 1986. Geochemistry and geochronology of the Kibaran granites in Burundi, Central Africa: Implications for the Kibaran Orogeny. Chemical Geology, 57, 217-234.

Fernandez-Alonso, M., De Waele, B., Tahon, A., Dewaele, S., Baudet, D., Cutten, H. and Tack, L., 2009. The Northeastern Kibaran Belt (NKB): a 1250 Ma-long Proterozoic intracratonic history in Central Africa punctuated by two orogenic events at c. 1.0 and 0.55 Ga. Rodinia: Supercontinents, Superplumes and Scotland. Geol. Soc. London Fermor Meeting, Edinburgh, Scotland, 6-13 September 2009, Abstracts vol., p. 22.

Fernandez-Alonso, M., Cutten, H., De Waele, B., Baudet, D., Tahon, A. and Tack, L., in prep. i*n* Gondwana Research. The Karagwe-Ankole belt (KAB): a 1250 Ma-long Proterozoic intra-cratonic history in Central Africa.

Gérards, J. et Ledent, D., 1970. Grands traits de la géologie du Rwanda, différents types de roches granitiques et premières données sur l'âge de ces roches. Annales Société Géologique Belgique, 93, 477-489.

Gosse, R., 1992. The Kabanga Ni-(Co-Cu) sulphide deposit, western Tanzania. IGCP No 255 Bulletin / Newsletter 4 (TU Braunschweig and RMCA, Tervuren), 73-76.

Griffin, W.L., Pearson, N.J., Belousova, E., Jackson, S.E., van Achterbergh, E., O'Reilly, S.Y. and Shee, S.R., 2000. The Hf isotope composition of cratonic mantle: LAM-MC-ICPMS analysis of zircon megacrysts in kimberlites. Geochimica et Cosmochimica Acta, 64, 133-147.

Griffin, W.L., Belousova, E.A., Shee, S.R., Pearson, N.J. and O'Reilly, S.Y., 2004. Archean crustal evolution in the northern Yilgarn Craton: U-Pb and Hf-isotope evidence from detrital zircons., Precambrian Research, 131, 231-282.

Hanson, R., Harmer, R., Blenkinsop, T., Bullen, D., Dalziel, I., Gose, W., Hall., Kampunzu, A., Key, R., Mukwakwami, J., Munyanyiwa, H., Pancake, J., Seidel, E. and Ward, S., 2006. Mesoproterozoic intraplate magmatism in the Kalahari Craton: A review. Journal of African Earth Sciences, 46, 141-167.

Henk, A., Franz, L., Teufel, S. and Oncken, O., 1997. Magmatic underplating, extension and crustal reequilibration: insights from a Cross-Section through the Ivrea Zone and Strona-Ceneri Zone, Northern Italy. Journal of Geology, 105, 367-377.

Hester, B., Barnard, F. and Johnson, A., 1991. Tanzania. Opportunities for Mineral Resource Development. Ministry of Water, Energy and Minerals, United Republic of Tanzania, 108 pp.

Ikingura, J.R., Bell, K., Watkinson, D.H. and Van Straaten, P., 1990. Geochronology and Chemical evolution of Granitic Rocks, NE Kibaran (Karagwe-Ankolean) Belt, NW

Tanzania., *in* Rocci, G., and Deschamps, M. editors, $15^{th}$ Colloquium of African Geology: Nancy, France, International Center for Training and Exchanges in the Geosciences (CIFEG), 97-99.

Ikingura, J.R., Reynolds, P.H., Watkinson, D.H. and Bell, K., 1992. Ar-Ar dating of micas from granites of NE Kibaran Belt (Karagwe-Ankolean), NW Tanzania. Journal of African Earth Sciences, 15, 501-511.

Johnson, S., De Waele, B. and Liyungu, K., 2006. U-Pb sensitive high-resolution ion microprobe (SHRIMP) zircon geochronology of granitoid rocks in eastern Zambia: Terrane subdivision of the Mesoproterozoic Southern Irumide Belt. Tectonics, 25, TC6004, doi:10.1029/2006TC001977.

Kampunzu, A.B., Rumvegeri, B.T., Kapenda, D., Lubala, R.T. and Caron, J.P.H., 1986. Les Kibarides d'Afrique centrale et orientale: une chaîne de collision. UNESCO, Geology for Development Newsletter, 5, 125-137.

Kampunzu, A.B., 2001. Assembly and break-up of Rodinia - no link with Gondwana assembly. Gondwana Research, 4, 647-650.

Klerkx, J., Liégeois, J.P., Lavreau, J. and Theunissen, K., 1984. Granitoides kibariens précoces et tectonique tangentielle au Burundi: magmatisme bimodal lié a une distention crustale, *in* Klerkx, J. and Michot, J. (Editors), African Geology, a Volume in honour of L. Cahen. Royal Museum for Central Africa, Tervuren, 29-46.

Klerkx, J., Liégeois, J.-P., Lavreau, J. and Claessens, W., 1987. Crustal evolution of the northern Kibaran Belt, eastern and central Africa, *in* Kröner, A. (Editor), Proterozoic Lithospheric Evolution, American Geophysical Union and the Geological Society of America, 17, 217-233.

Klerkx, J., Theunissen, K. and Delvaux, D., 1998. Persistent fault controlled basin formation since the Proterozoic along the Western Branch of the East African Rift. Journal of African Earth Sciences, 26, 347-361.

Kokonyangi, J., 2001. Geological Fieldwork in the Kibaran-Type Region, Mitwaba District, Congo (former Zaire), Central Afric. Gondwana Research, 4, 255-259.

Kokonyangi, J., Armstrong, R.A., Kampunzu, A.B. and Yoshida, M., 2001a. SHRIMP U-Pb zircon geochronology of granitoids in the Kibaran type area, Mitwaba-Central Katanga (Congo). Gondwana Research, 4, 661-663.

Kokonyangi, J., Okudiaira, T., Kampunzu, A.B. and Yoshida, M., 2001b. Geological evolution of the Kibarides belt, Mitwaba, Democratic Republic of Congo, central Afric. Gondwana Research, 4, 663-664.

Kokonyangi, J., Armstrong, R.A., Kampunzu, A.B., Yoshida, M. and Okudaira, T., 2002. Magmatic evolution of the Kibarides belt (Katanga, Congo) and implications for Rodinia reconstruction: Field observations, U-Pb SHRIMP geochronology and geochemistry of granites, *in* Namibia G.S.A. editor, $11^{th}$ IAGOD Quadrennial Symposium and Geocongress. Windhoek, Namibia, Geological Survey of Namibia, 5 pp.

Kokonyangi, J., Armstrong, R.A., Kampunzu, A.B., Yoshida, M. and Okudaira, T., 2004a. U–Pb zircon geochronology and petrology of granitoids from Mitwaba (Katanga, Congo): implications for the evolution of the Mesoproterozoic Kibaran belt. Precambrian Research, 132, 79-106.

Kokonyangi, J., Kampunzu, A.B., Armstrong, R., Yoshida, M. and Okudaira, T., 2004b. Mesoproterozoic evolution of the Kibaride (Congo, Central Africa): Geotectonic implications, $32^{nd}$ International Geological Congress, Florence, Italy, p. 875.

Kokonyangi, J., Kampunzu, A.B., Poujol, M., Okudaira, T., Yoshida, M. and Shabeer, K.P., 2005. Petrology and geochronology of Mesoproterozoic mafic–intermediate plutonic rocks from Mitwaba (D. R. Congo): implications for the evolution of the Kibaran belt in central Afric. Geological Magazine, 142, 109-130.

Kokonyangi, J., Kampunzu, A.B., Armstrong, R., Yoshida, M., Okudaira, T., Arima, M. and Ngulube, D.A., 2006. The Mesoproterozoic Kibaride belt (Katanga, SE D.R. Congo). Journal of African Earth Sciences, 46, 1-35.

Kokonyangi, J., Kampunzu, A., Armstrong, R., Arima, M., Yoshida, M. and Okudaira, T., 2007. U-Pb SHRIMP dating of detrital zircons from the Nzilo Group (Kibaran Belt): Implications for the source of sediments and Mesoproterozoic evolution of Central Africa. Journal of Geology, 115, 99-113.

Kokonyangi, J., Dunkley, D., Bulambo, M., Francart, J.P., Itaya, T., Arima, M. and Yoshida, M., 2008. First Cassiterite SHRIMP *vs* K-Ar geochronology on tin and Nb-Ta mineralization in the Kibaran Belt: implications to Rodinia and Gondwana tectonics. 22$^{nd}$ Colloquium African Geology (CAG22), 04-06.11.2008, Hammamet, Tunisia, Abstract volume, p. 250.

Lavreau, J., 1985. Le Groupe de la Rusizi (Rusizien du Zaïre, Rwanda et Burundi) à la lumière des connaissances actuelles. Royal Museum for Central Africa, Tervuren (Belgium), Dépt. Géologie Minéralogie, Ann. Rep. 1984, 111-119.

Lavreau, J. et Liégeois, J.P., 1982. Granites à étain et granito-gneiss burundiens au Rwanda (région de Kibuye): âge et signification. Annales Société Géologique Belgique, 105, 289-294.

Ledent, D., 1979. Données géochronologique relatives aux granites Kibariens de types A (ou G1) et B (ou G2) du Shaba, du Rwanda, du Burundi et du SW Uganda. Royal Museum for Central Africa, Tervuren (Belgium), Dépt. Géologie Minéralogie, Ann. Rep. 1978, 101-105.

Lepersonne, J., 1974. Carte géologique du Zaïre au 1/2 000 000 et notice explicative, République du Zaïre, Département des Mines, Direction de la Géologie, 67 pp.

Li, Z. X., Bogdanova, S., Collins, A., Davidson, A., De Waele, B., Ernst, R., Fitzimons, I., Fuck, R., Gladkochub, D., Jacobs, J., Karlstrom, K., Lu, S., Natapov, L., Pease, V., Pisarevsky, S., Thrane, K. and Vernikovsky, V., 2008. Assembly, configuration and break-up history of Rodinia: A synthesis. Precambrian Research, 160, 179-210.

Maier, W.D., Peltonen, P. and Livesey, T., 2007. The ages of the Kabanga North and Kapalagulu intrusions, Western Tanzania: a reconnaissance study. Economic Geology, 102, 147-154.

Master, S., Bekker, A. and Karhu, J.A., 2008. Palaeoproterozoic high delta13 carb marbles from the Ruwenzori Mountains, Uganda, and implications for the age of the Buganda-Toro Supergroup, 22$^{nd}$ Colloquium of African Geology, Hammamet, Tunisia, p. 90.

Mayer, A., Hofmann, A.W., Sinigoi, S. and Morais, E., 2004. Mesoproterozoic Sm–Nd and U–Pb ages for the Kunene Anorthosite Complex of SW Angola. Precambrian Research, 133, 187-206.

McCourt, S., Armstrong, R., Grantham, G. and Thomas, R., 2006. Geology and evolution of the Natal belt, South Africa. Journal of African Earth Sciences, 46, 71-92.

McLaren, A.,C., Fitzgerald, J. and Williams, I., 1994. The microstructure of zircon and its influence on the age determination from Pb/U isotopic ratios measured by ion microprobe. Geochemica et Cosmochemica Acta, 58, 993-1005.

Meert, J.G., Hargraves, R.B., Van, d.V.R., Hall, C.M. and Halliday, A.N., 1994a. Paleomagnetic and $^{40}$Ar/$^{39}$ Ar studies of late Kibaran intrusives in Burundi, east Africa; implications for late Proterozoic supercontinents. Journal of Geology, 102, 621-637.

Meert, J.G., Uranga, C., Van, d.V.R., Ayub, S. and Munyua, R., 1994b. Middle and late Proterozoic paleomagnetic results from the Congo Craton. In: Anonymous (Editor), AGU 1994 spring meeting. American Geophysical Union, Washington, DC, United States.

Nahimana, L., 1988. Métamorphisme, tectonique et magmatisme dans une portion de la chaîne kibarienne du Nord-Ouest du Burundi, PhD Thesis (unpublished), Université Catholique de Louvain-la-Neuve (Belgium), Louvain La Neuve, 206 pp.

Nahimana, L. and Tack, L., unpublished data.

Nelson, D.R., 1997. Compilation of SHRIMP U-Pb zircon geochronology data, 1996. Geological Survey of Western Australia, Record 1997/2, Geological Survey of Western Australia, Perth, Australia, p. 189.

Ntungicimpaye, A., 1984. Contribution à l'étude du magmatisme basique dans le Kibarien de la partie occidentale du Burundi, PhD Thesis (unpublished), University of Ghent (Belgium), 250 pp.

Ntungicimpaye, A. and Kampunzu, A.B., 1987. Caracterisation Geochimique des Metabasites Kibariennes (Proterozoique Moyen) du Burundi, *in* Matheis, G. and Schandelmeier, H. (Editors), 14th Colloquium of African Earth Sciences. Balkema, Berlin, p. 37-40.

Nzojibwami, E., 1987. Le Précambrien cristallin de la région de Bujumbura (Burundi), PhD Thesis (unpublished), Université de Liège (Belgium), 232 pp.

Pidgeon, R.T., Furfaro, D., Kennedy, A.K., Nemchin, A.A. and Van Bronswijk, W., 1994. Calibration of zircon standards for the Curtin SHRIMP II. United States Geological Survey circular, 1107, p. 251.

Pohl, W., 1994. Metallogeny of the northeastern Kibaran belt, central Africa - recent perspectives. Ore Geology Reviews, 9, 105-130.

Romer, R.L. and Lehmann, B., 1995. U-Pb columbite age of Neoproterozoic Ta-Nb mineralization in Burundi. Economic Geology and the Bulletin of the Society of Economic Geologists, 90, 2303-2309.

Rumvegeri, B.T., 1991. Tectonic significance of Kibaran structures in Central and eastern Afric. Journal of African Earth Sciences, 13, 267-276.

Rumvegeri, B.T., Bingen, B. and Derron, M.H., 2004. Tectonomagmatic evolution of the Kibaran Belt in Central Africa and its relationships with mineralizations; a review. Africa Geoscience Review, 11, 65-73.

Stacey, J.S. and Kramers, J.D., 1975. Approximation of terrestrial lead isotopic evolution by a two-stage model. Earth and Planetary Science Letters, 26, 207-221.

Steiger, R.H. and Jäger, E., 1977. Subcommission on geochronology: convention on the use of decay constants in geo- and cosmochronology. Earth and Planetary Science Letters, 36, 359-362.

Tack, L., 1995. The Neoproterozoic Malagarazi Supergroup of SE Burundi and its equivalent Bukoban System in NW Tanzania; a current review, in: Wendorff, M. and Tack, L. (Editors), Late Proterozoic belts in Central and Southwestern Africa; IGCP Project 302. Royal Museum for Central Africa, Tervuren (Belgium), Geological Sciences, 101, 121-129.

Tack, L., De Paepe, P., Deutsch, S. and Liégeois, J.P., 1984. The alkaline plutonic complex of the Upper Ruvubu (Burundi): geology, age, isotopic geochemistry and implications for the regional geology of the Western Rift, *in* Klerkx, J. and Michot, J. (Editors), African Geology, A volume in honour of L. Cahen. Musée Royal d'Afrique Centrale, Tervuren (Belgium), 91-114.

Tack, L., De Paepe, P., Liégeois, J.P., Nimpagaritse, G., Ntungicimpaye, A. and Midende, G., 1990. Late Kibaran magmatism in Burundi. Journal of African Earth Sciences, 10, 733-738.

Tack, L., Sindayihebura, L., Cimpaye, D., 1992. The Nkoma (SE Burundi): an episodically reactivated lower Burundian siliciclastic sequence, locally overlain by a Malagarasian sedimentary breccia. IGCP No 255 Newsletter / Bulletin 4 (TU Braunschweig and RMCA, Tervuren), 9-22.

Tack, L., Liégeois, J.P., Deblond, A. and Duchesne, J.C., 1994. Kibaran A-type granitoids and mafic rocks generated by two mantle sources in a late orogenic setting (Burundi). Precambrian Research, 68, 323-356.

Tack, L., Liégeois, J.-P., Deblond, A. and Duchesne, J.-C., 1995. The Kibaran Event in Africa: a need for redefinition. Centenial Geocongress, Geol. Soc. S. Afr., Johannesburg, South-Africa, Extended Abstracts volume, 402-405.

Tack, L., Baudet, D., Chartry, G., Deblond, A., Fernandez-Alonso, M., Lavreau, J., Liégeois, J.-P., Tahon, A., Theunissen, K, Trefois, Ph. and Wingate, M., 2002a. The Northeastern Kibaran Belt (NKB) reconsidered: evidence for a c. 1370 Ma-old, repeatedly reactivated Kibara mobile belt, preceding the c. 1.0 Ga Rodinia Supercontinent assembly. 19th Colloquium of African Geology, El Jadida, Morocco, 19-23 March 2002, Special Abstracts volume, p. 173.

Tack, L., Fernandez-Alonso, M., Tahon, A., Wingate, M. and Barritt, S., 2002b. The "Northeastern Kibaran Belt" (NKB) and its mineralisations reconsidered: new constraints from a revised lithostratigraphy, a GIS-compilation of existing geological maps and a review of recently published as well as unpublished igneous emplacement ages in Burundi. - 11th Quadrennial IAGOD Symposium and GEOCONGRESS 2002, 22-26 July, Windhoek, Namibia, Synopsis of Extended Abstract (on CD-Rom), Conference Programme volume, p. 42.

Tack, L., Fernandez-Alonso, M., De Waele, B., Tahon, A., Dewaele, S., Baudet, D. and Cutten, H., 2006. The Northeastern Kibaran Belt (NKB): a long-lived Proterozoic intraplate history. 21st Colloquium African Geology (CAG21), 03-05.07.2006, Maputo, Mozambique, Abstract volume, 149- 151.

Tack, L., Wingate, M., De Waele, B., Meert, J., Griffin, B., Belousova, E.A., Tahon, A., Fernandez-Alonso, M., Baudet, D., Cutten, H., Dewaele, S.. 2008. The Proterozoic Kibaran Belt in Central Africa: intra-cratonic 1375 Ma emplacement of a LIP. 22nd Colloquium African Geology (CAG22), 04-06.11.2008, Hammamet, Tunisia, Abstract volume, p. 89.

Tahon, A., Fernandez-Alonso, M, Tack, L. and Barritt, S., 2004. New insights about the evolution of the Mesoproterozoic Northeastern Kibaran belt (Central Africa) – 20th Colloquium on African Geology, Orléans, June 2004, Abstracts volume, p. 389.

Theunissen, K., 1988. Kibaran thrust fold belt ($D_{1-2}$) and shear belt ($D_{2'}$). IGCP No 255 Bulletin / Newsletter 1 (TU Braunschweig and RMCA, Tervuren), 55-64.

Theunissen, K., 1989. On the Rusizian basement rise in the Kibara Belt of Northern Lake Tanganyika. Collision belt geometry or restraining bend emplaced in the late Kibaran strike-slip environment. IGCP No 255 Bulletin / Newsletter 2 (TU Braunschweig and RMCA, Tervuren), 85-92.

Theunissen, K., Hanon, M. and Fernandez-Alonso, M., 1991. Carte Géologique du Rwanda, 1:200.000. Service Géologique, Ministère de l'Industrie et de l'Artisanat, République Rwandaise.

Theunissen, K., Klerkx , J., Melnikov, A. and Mruma, A., 1996. Mechanisms of inheritance of rift faulting in the western branch of the East African Rift, Tanzania. Tectonics, 15, 776-790.

Theunissen, K., Boven, A., Punzalan, L., personal communication: Amphibole and biotite $^{40}Ar/^{39}Ar$ ages in the Ubende Belt (Tanzania) and link with the Kibara Belt evolution, unpublished abstract, 1p.

Villeneuve, M. et Guyonnet-Benaize, C., 2006. Apports de l'imagerie spatiale à la résolution des structures géologiques en zone équatoriale: exemples du Précambrien au Kivu (Congo Oriental). Photo-Interprétation, 4, 3-22 et 59-67.

Wadsworth, W.J., Dunham, A.C. and Almohandis, A.A., 1982. Cryptic variation in the Kapalagulu layered intrusion, western Tanzania. Mineralogical Magazine, 45, 227-236.

Walemba, K.M.A., 2001. Geology, geochemistry and tectono-metallogenic evolution of Neoproterozoic gold deposits in the Kadubu area, Kivu, Democratic Republic of Congo. Ph. D. Thesis (unpublished), University of the Witwatersrand, Johannnesburg, South Africa, 491 pp.

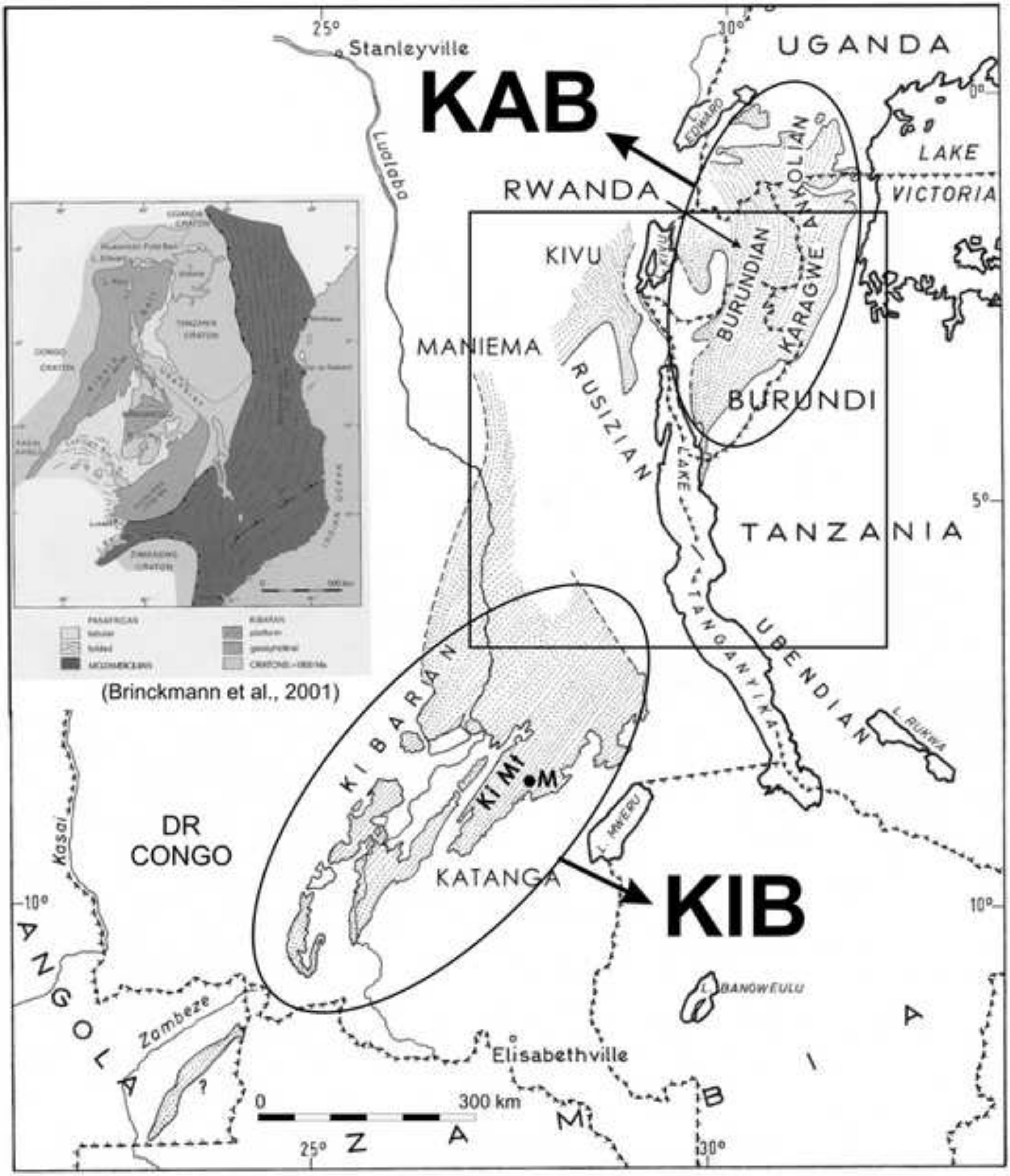
KAB
KIB
UGANDA
LAKE
VICTORIA
RWANDA
KIVU
MANIEMA
RUSIZIAN
BURUNDIAN
KARAGWE ANKOLIAN
BURUNDI
TANZANIA
LAKE TANGANYIKA
UBENDIAN
L. RUKWA
KIBARAN
Ki Mt
M
L. MWERU
DR
CONGO
KATANGA
ANGOLA
Kasai
Lualaba
Zambeze
Stanleyville
Elisabethville
L. BANGWEULU
ZAMBIA
0
300 km
25°
30°
5°
10°
(Brinckmann et al., 2001)

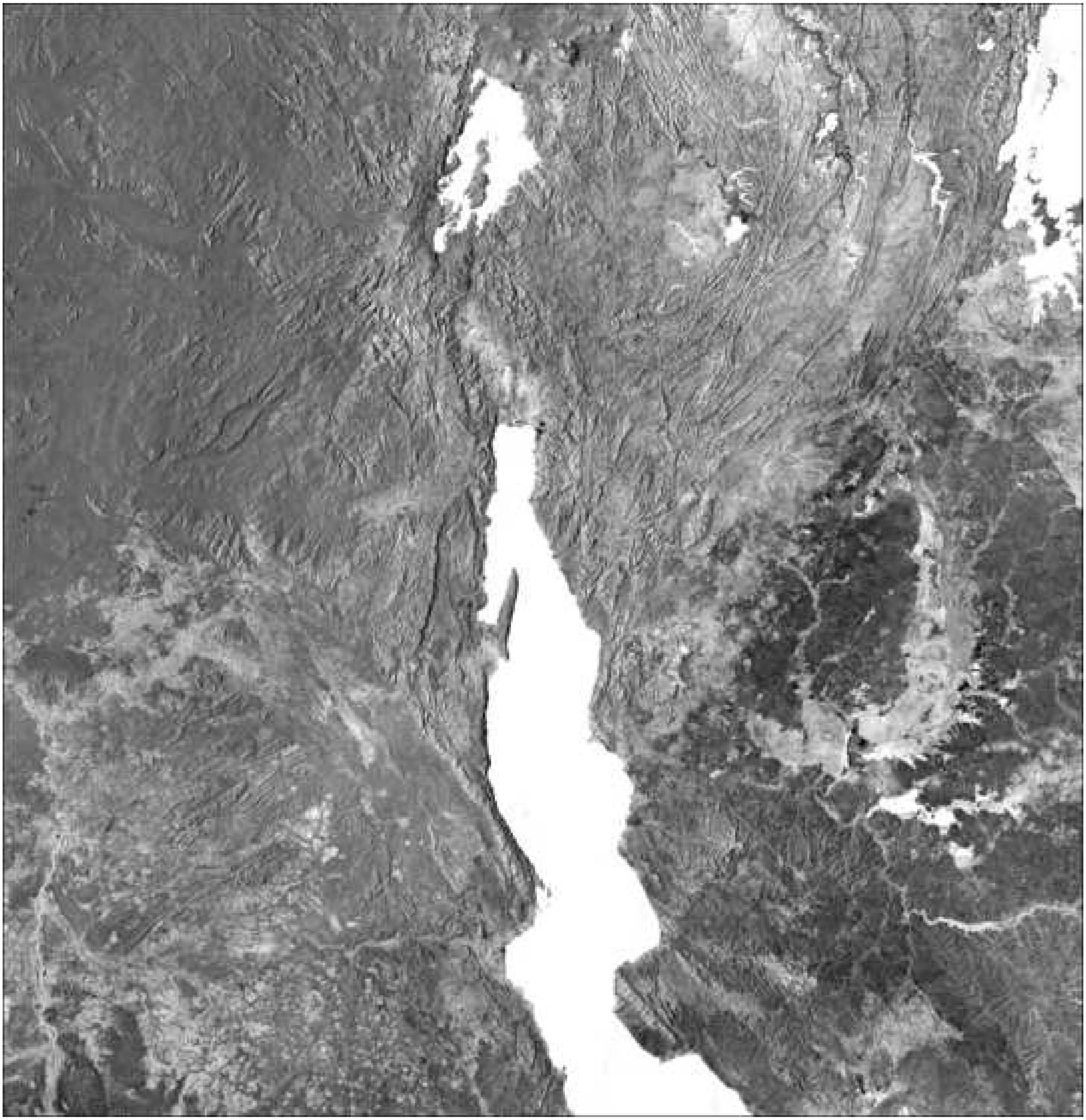

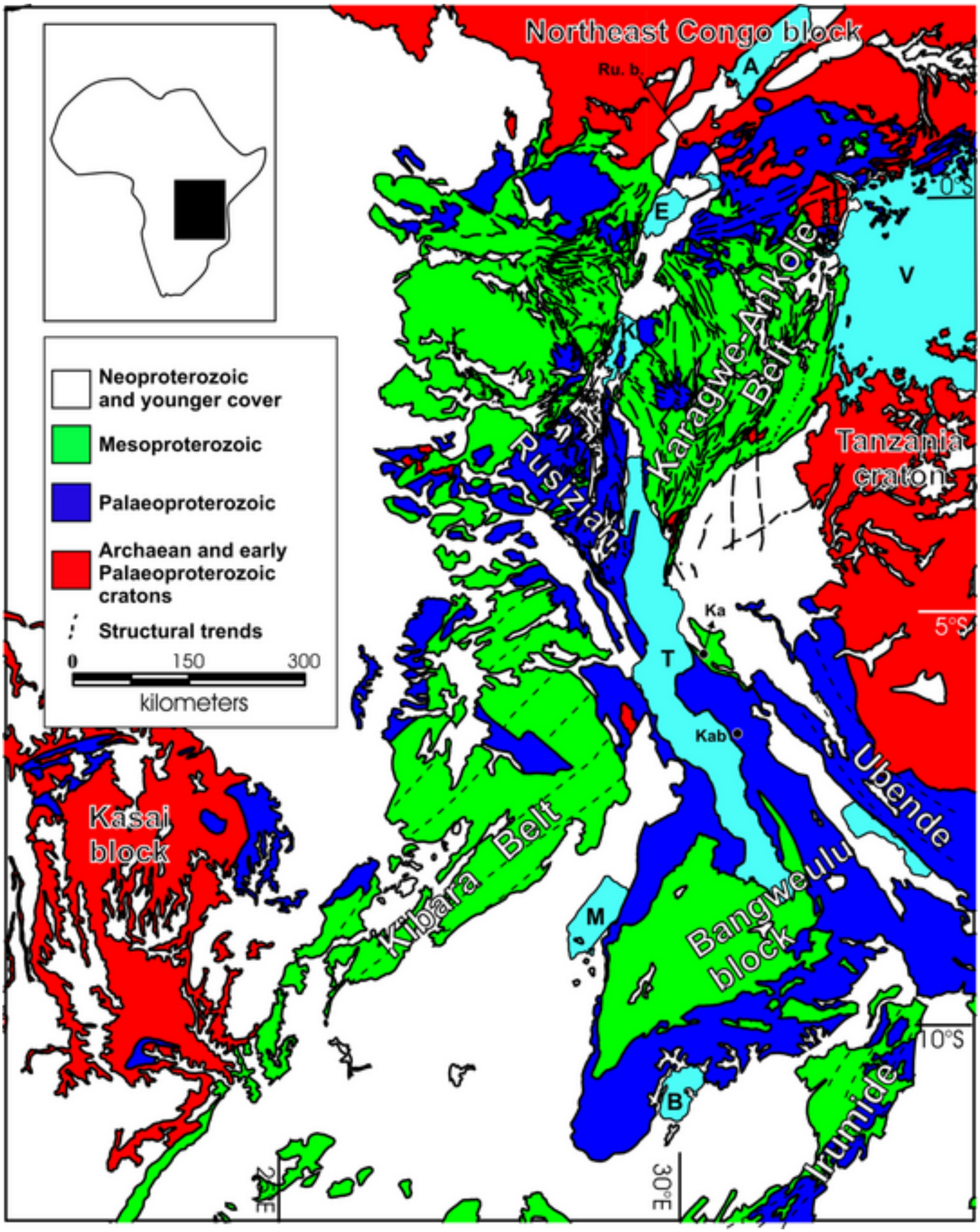
Northeast Congo block
Ru. b.
A
E
V
0°S
K
Karagwe-Ankole Belt
Tanzania craton
Rusizian
Ka
T
5°S
Kab
Ubende
Kasai block
Kibara Belt
Bangweulu block
M
10°S
B
Irumide
30°E
Neoproterozoic and younger cover
Mesoproterozoic
Palaeoproterozoic
Archaean and early Palaeoproterozoic cratons
Structural trends
0
150
300
kilometers

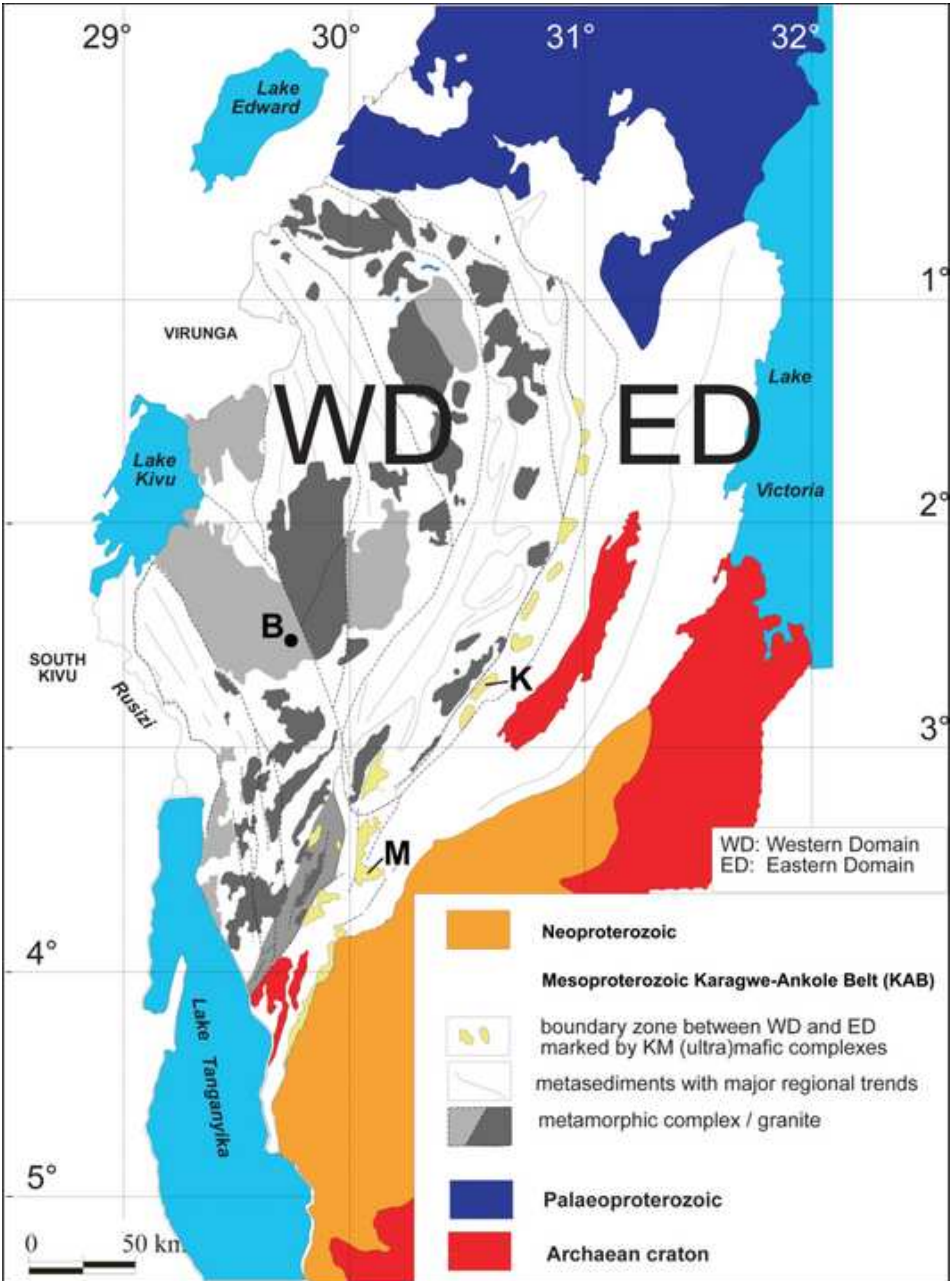
29°
30°
31°
32°
1°
2°
3°
4°
5°
Lake Edward
VIRUNGA
WD
ED
Lake Victoria
Lake Kivu
B
SOUTH KIVU
Rusizi
K
M
Lake Tanganyika
WD: Western Domain
ED: Eastern Domain
Neoproterozoic
Mesoproterozoic Karagwe-Ankole Belt (KAB)
boundary zone between WD and ED marked by KM (ultra)mafic complexes
metasediments with major regional trends
metamorphic complex / granite
Palaeoproterozoic
Archaean craton
0
50 km

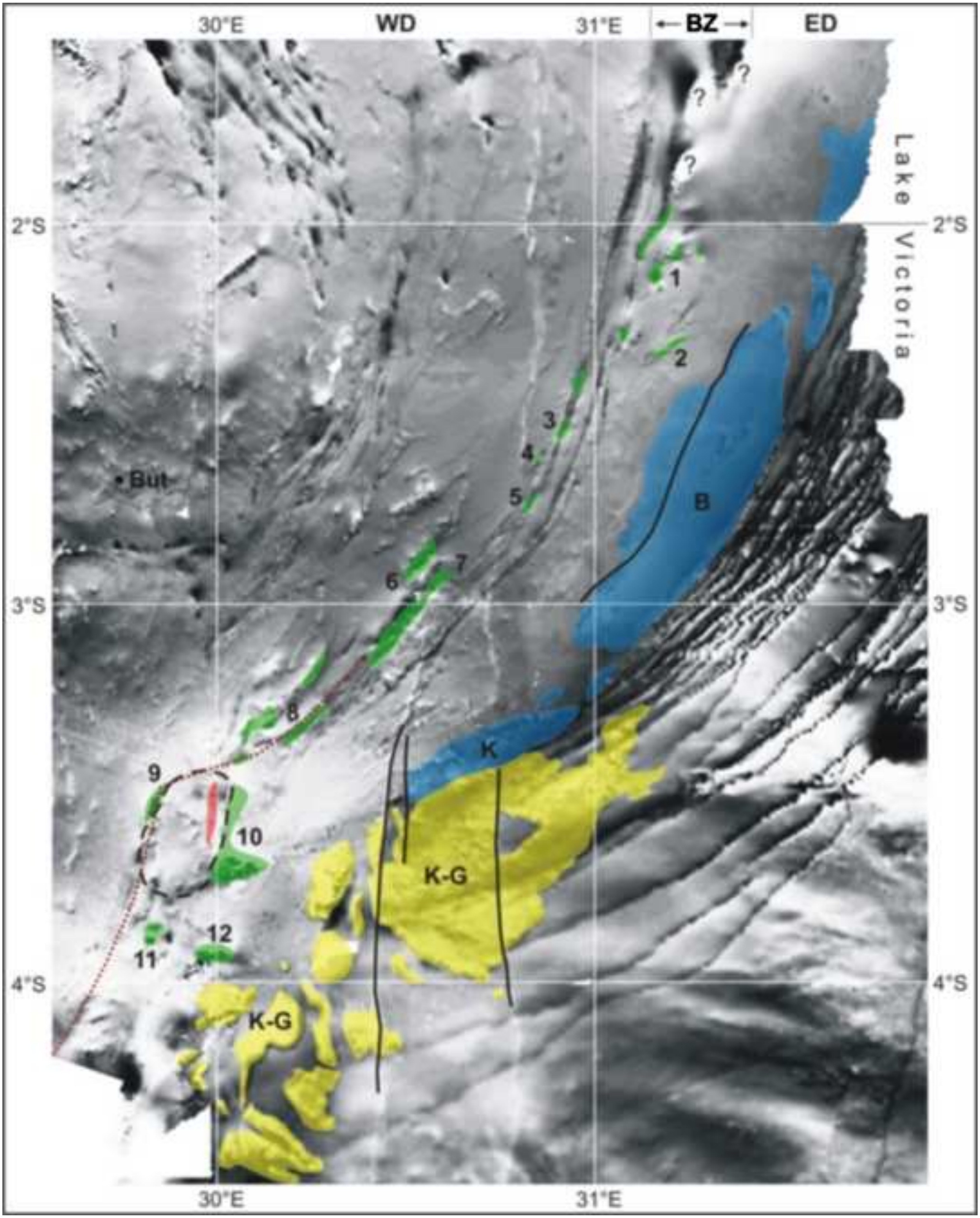
30°E
WD
31°E
BZ
ED
Lake Victoria
2°S
3°S
4°S
Bui
1
2
3
4
5
6
7
8
9
10
11
12
B
K
K-G
K-G

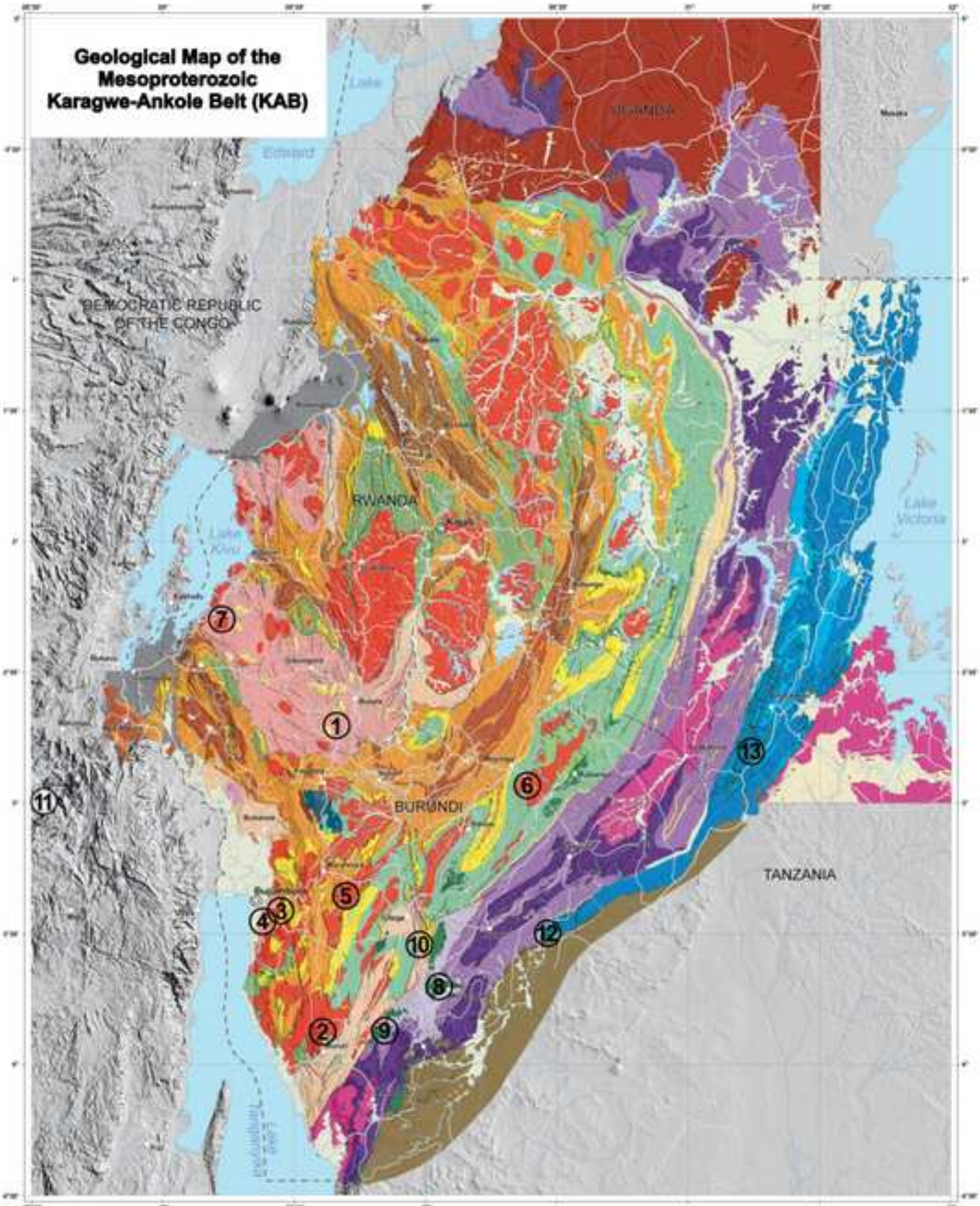
Geological Map of the
Mesoproterozoic
Karagwe-Ankole Belt (KAB)
UGANDA
DEMOCRATIC REPUBLIC
OF THE CONGO
RWANDA
BURUNDI
TANZANIA
Lake
Edward
Lake
Kivu
Lake
Victoria
Lake
Tanganyika
1
2
3
4
5
6
7
8
9
10
11
12
13

Figure6

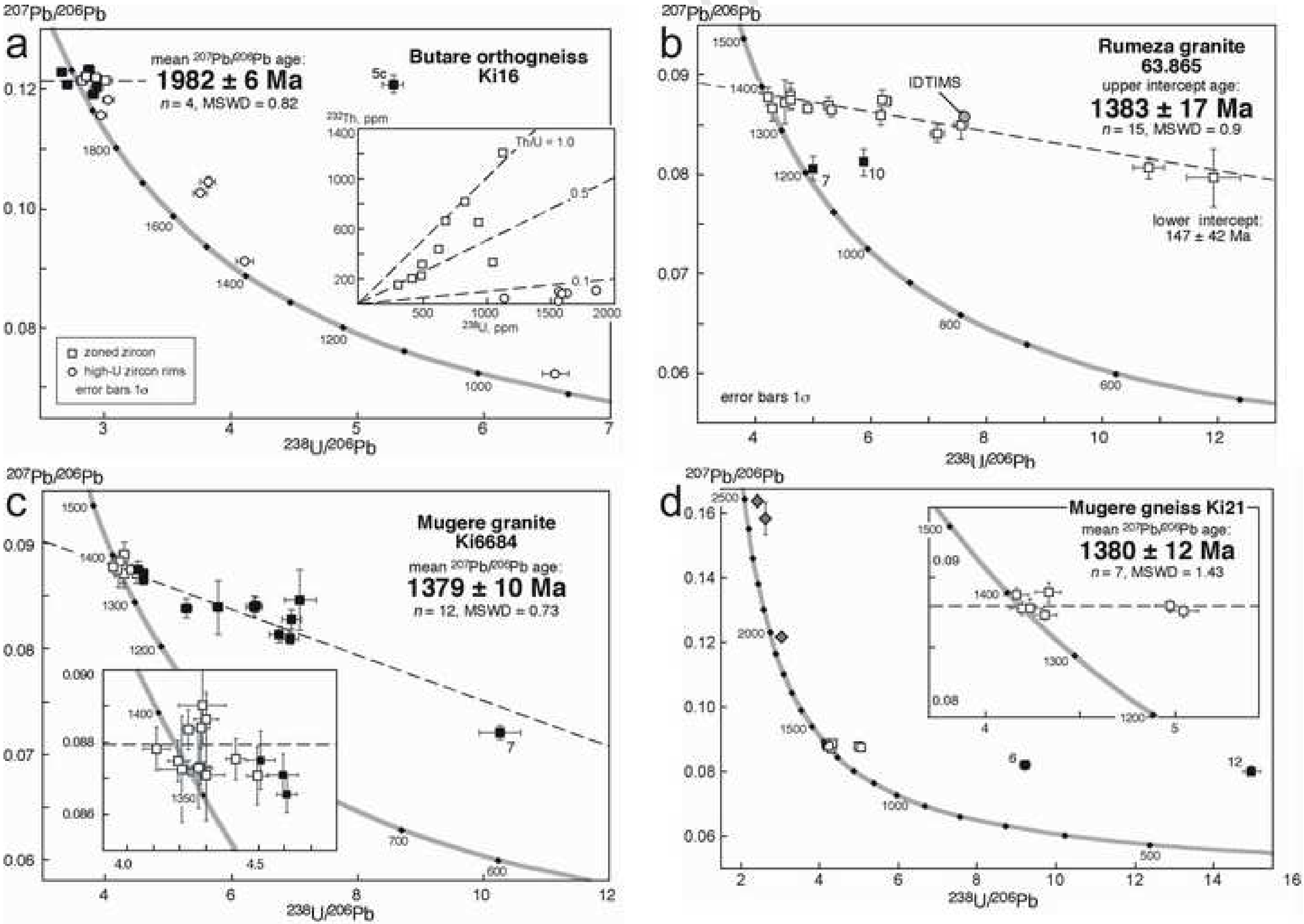
a
mean 207Pb/206Pb age:
1982 ± 6 Ma
n = 4, MSWD = 0.82
Butare orthogneiss
Ki16
zoned zircon
high-U zircon rims
error bars 1σ
b
Rumeza granite
63.865
upper intercept age:
1383 ± 17 Ma
n = 15, MSWD = 0.9
IDTIMS
lower intercept:
147 ± 42 Ma
error bars 1σ
c
Mugere granite
Ki6684
mean 207Pb/206Pb age:
1379 ± 10 Ma
n = 12, MSWD = 0.73
d
Mugere gneiss Ki21
mean 207Pb/206Pb age:
1380 ± 12 Ma
n = 7, MSWD = 1.43
238U/206Pb
207Pb/206Pb

Figure7

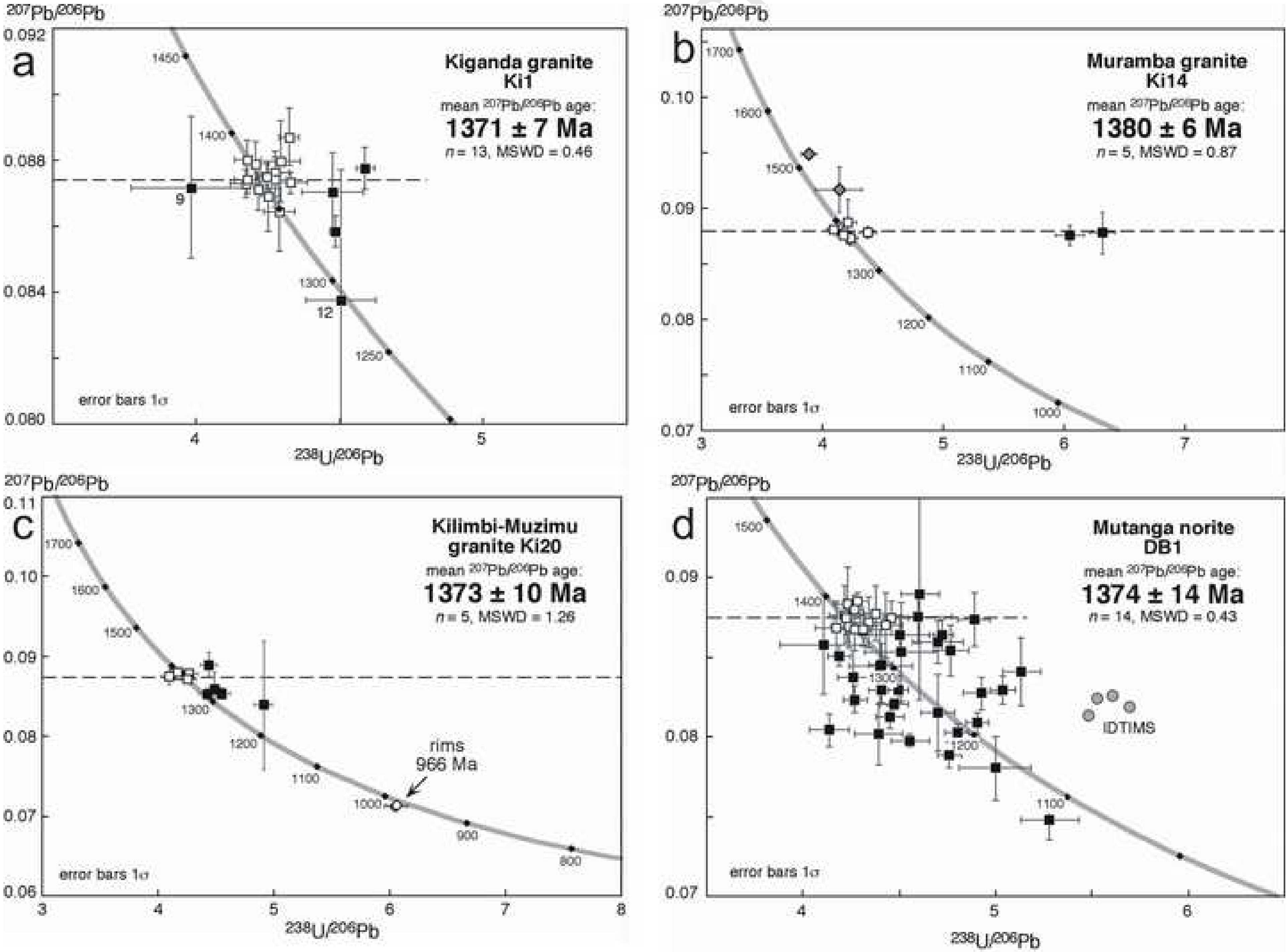

a
Kiganda granite
Ki1
mean $^{207}Pb/^{206}Pb$ age:
1371 ± 7 Ma
n = 13, MSWD = 0.46
error bars 1σ
$^{207}Pb/^{206}Pb$
$^{238}U/^{206}Pb$
b
Muramba granite
Ki14
mean $^{207}Pb/^{206}Pb$ age:
1380 ± 6 Ma
n = 5, MSWD = 0.87
error bars 1σ
c
Kilimbi-Muzimu
granite Ki20
mean $^{207}Pb/^{206}Pb$ age:
1373 ± 10 Ma
n = 5, MSWD = 1.26
rims
966 Ma
error bars 1σ
d
Mutanga norite
DB1
mean $^{207}Pb/^{206}Pb$ age:
1374 ± 14 Ma
n = 14, MSWD = 0.43
IDTIMS
error bars 1σ

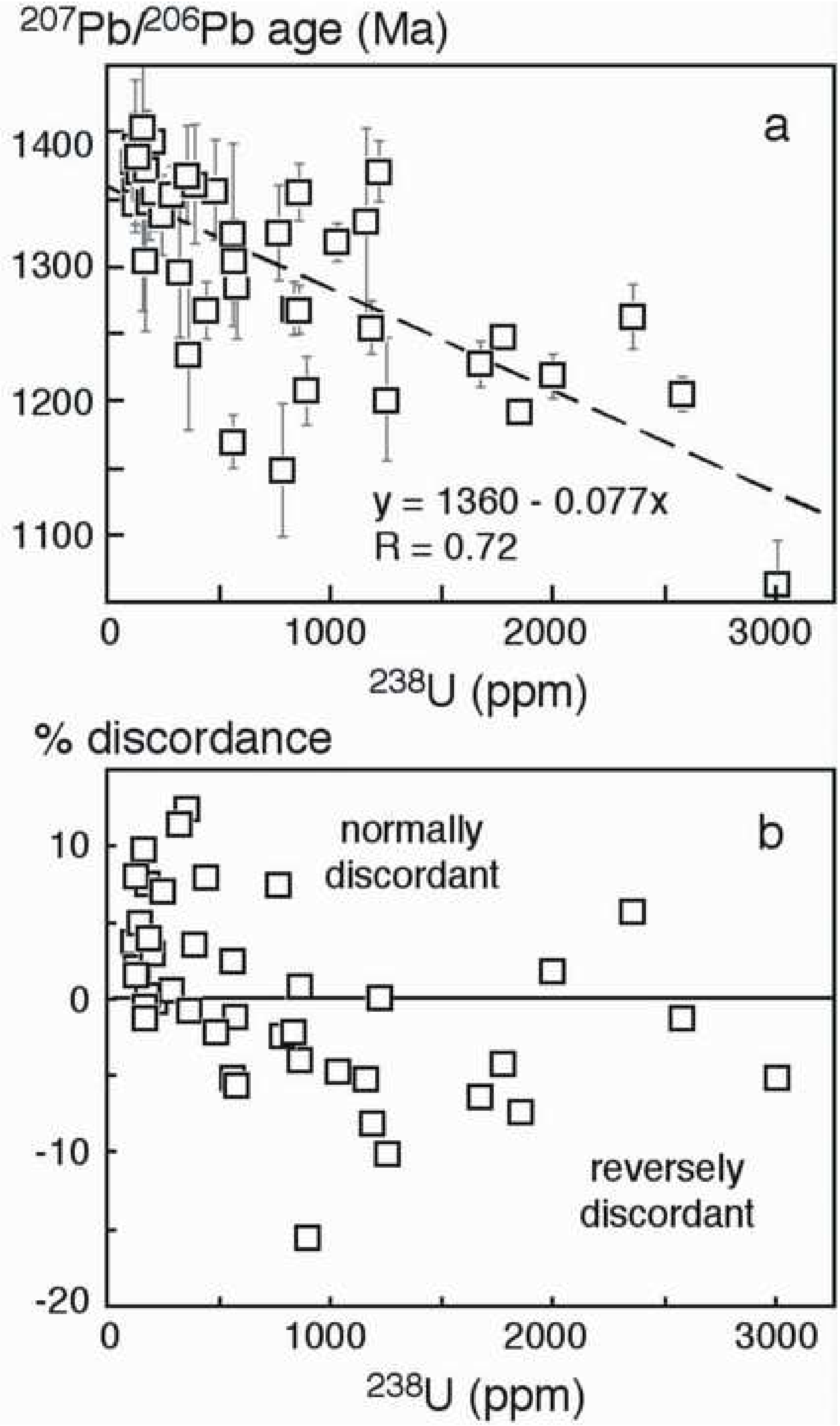
207Pb/206Pb age (Ma)
a
1400
1300
1200
1100
y = 1360 - 0.077x
R = 0.72
0
1000
2000
3000
238U (ppm)
% discordance
b
normally discordant
reversely discordant
10
0
-10
-20
0
1000
2000
3000
238U (ppm)

Figure9



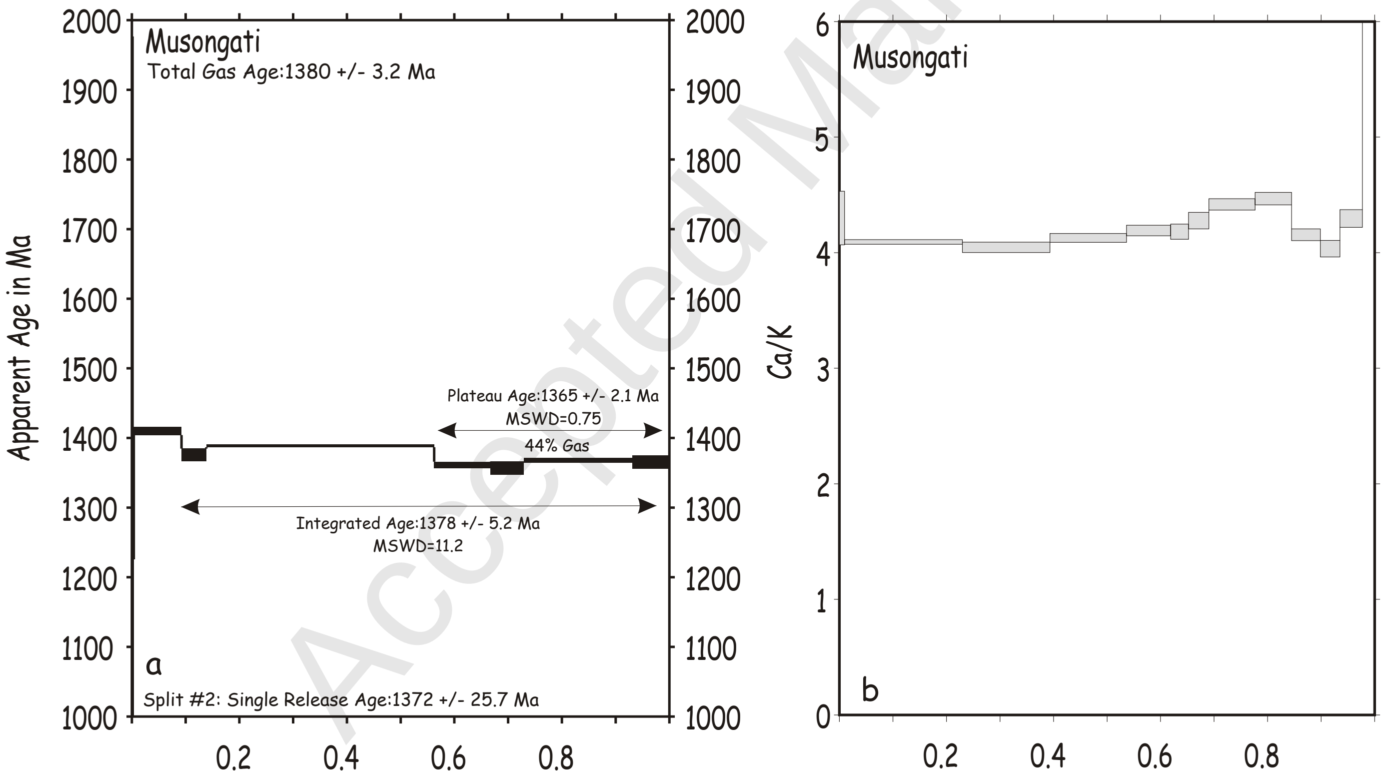
Musongati
Total Gas Age:1380 +/- 3.2 Ma
Plateau Age:1365 +/- 2.1 Ma
MSWD=0.75
44% Gas
Integrated Age:1378 +/- 5.2 Ma
MSWD=11.2
a
Split #2: Single Release Age:1372 +/- 25.7 Ma
Apparent Age in Ma
2000
1900
1800
1700
1600
1500
1400
1300
1200
1100
1000
0.2
0.4
0.6
0.8
Musongati
b
Ca/K
6
5
4
3
2
1
0

Figure10



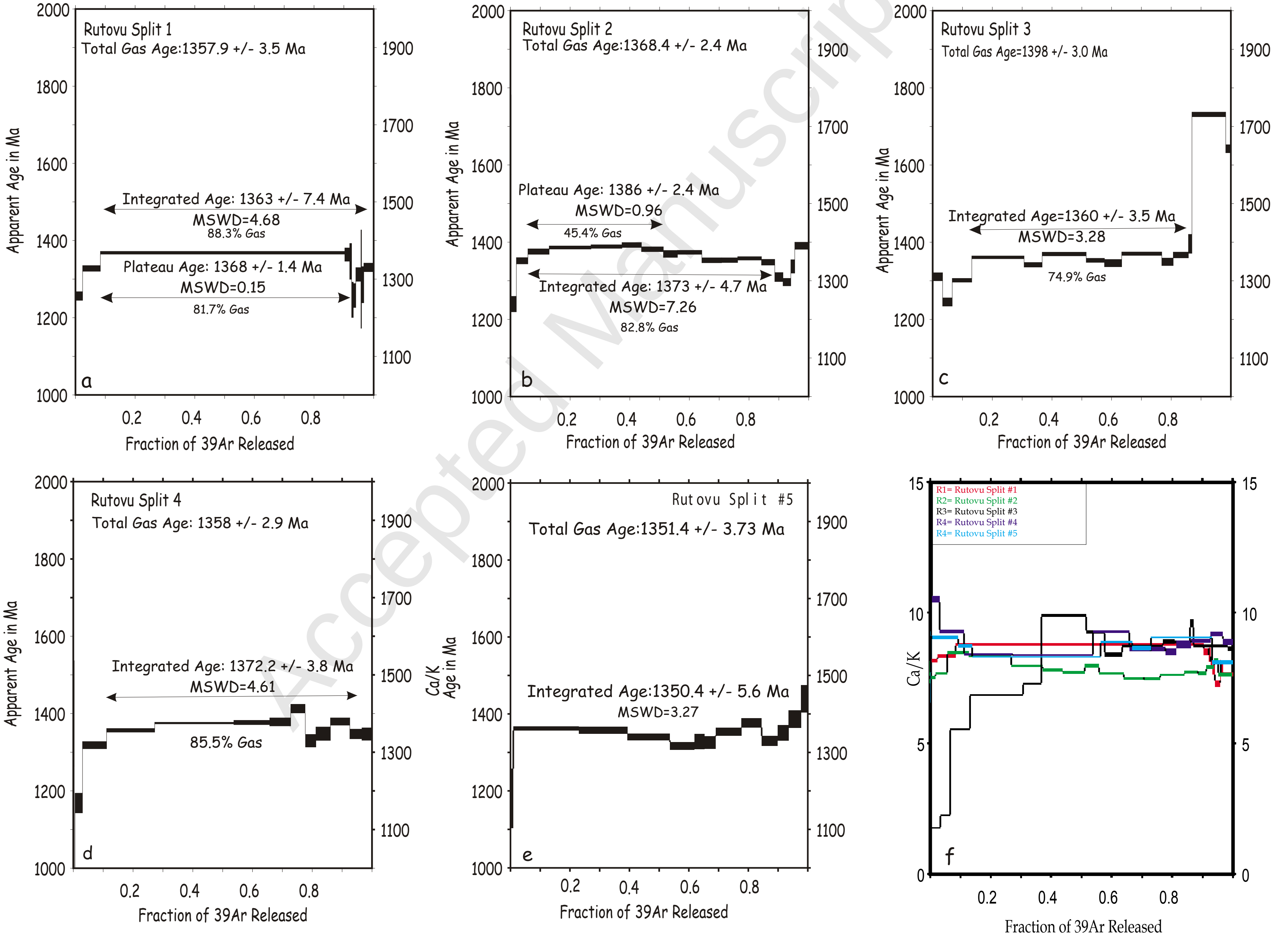

Rutovu Split 1
Total Gas Age:1357.9 +/- 3.5 Ma
Integrated Age: 1363 +/- 7.4 Ma
MSWD=4.68
88.3% Gas
Plateau Age: 1368 +/- 1.4 Ma
MSWD=0.15
81.7% Gas
a
Rutovu Split 2
Total Gas Age:1368.4 +/- 2.4 Ma
Plateau Age: 1386 +/- 2.4 Ma
MSWD=0.96
45.4% Gas
Integrated Age: 1373 +/- 4.7 Ma
MSWD=7.26
82.8% Gas
b
Rutovu Split 3
Total Gas Age=1398 +/- 3.0 Ma
Integrated Age=1360 +/- 3.5 Ma
MSWD=3.28
74.9% Gas
c
Rutovu Split 4
Total Gas Age: 1358 +/- 2.9 Ma
Integrated Age: 1372.2 +/- 3.8 Ma
MSWD=4.61
85.5% Gas
d
Rutovu Split #5
Total Gas Age:1351.4 +/- 3.73 Ma
Integrated Age:1350.4 +/- 5.6 Ma
MSWD=3.27
e
R1= Rutovu Split #1
R2= Rutovu Split #2
R3= Rutovu Split #3
R4= Rutovu Split #4
R4= Rutovu Split #5
f
Apparent Age in Ma
Ca/K Age in Ma
Ca/K
Fraction of 39Ar Released

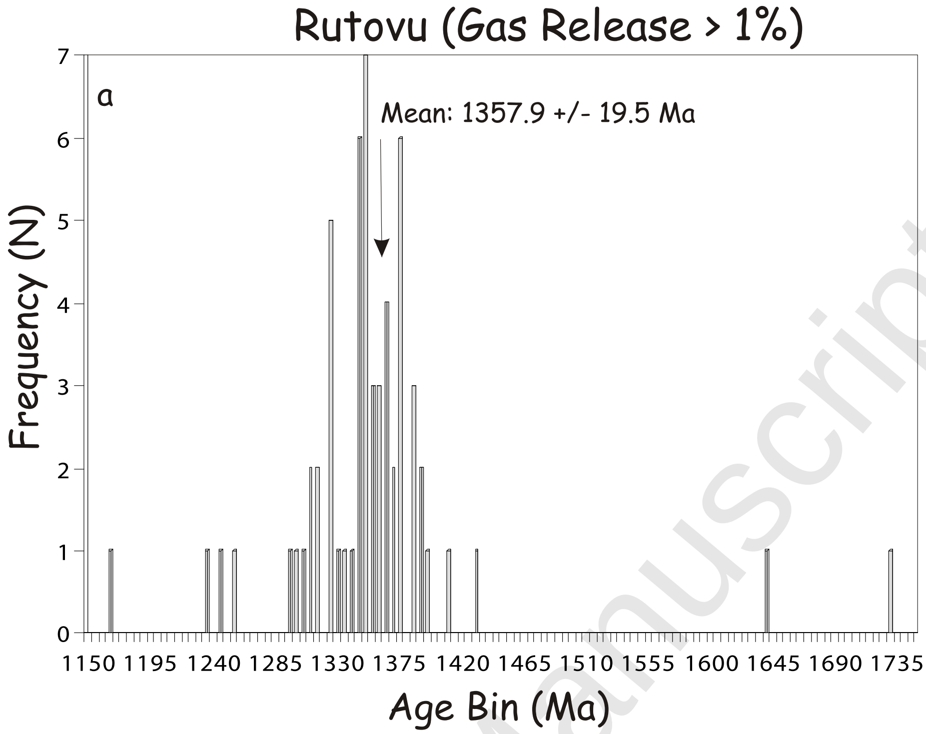
Rutovu (Gas Release > 1%)
a
Mean: 1357.9 +/- 19.5 Ma
Frequency (N)
0
1
2
3
4
5
6
7
1150 1195 1240 1285 1330 1375 1420 1465 1510 1555 1600 1645 1690 1735
Age Bin (Ma)

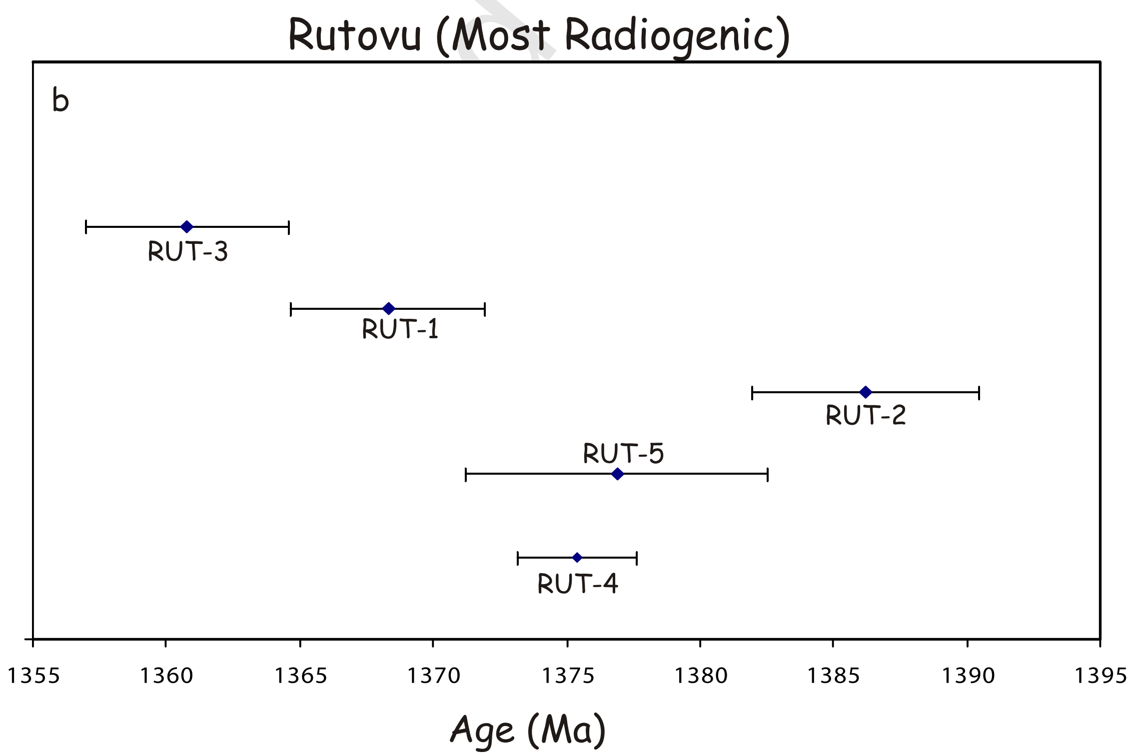
Rutovu (Most Radiogenic)
b
RUT-3
RUT-1
RUT-2
RUT-5
RUT-4
1355 1360 1365 1370 1375 1380 1385 1390 1395
Age (Ma)

Figure12



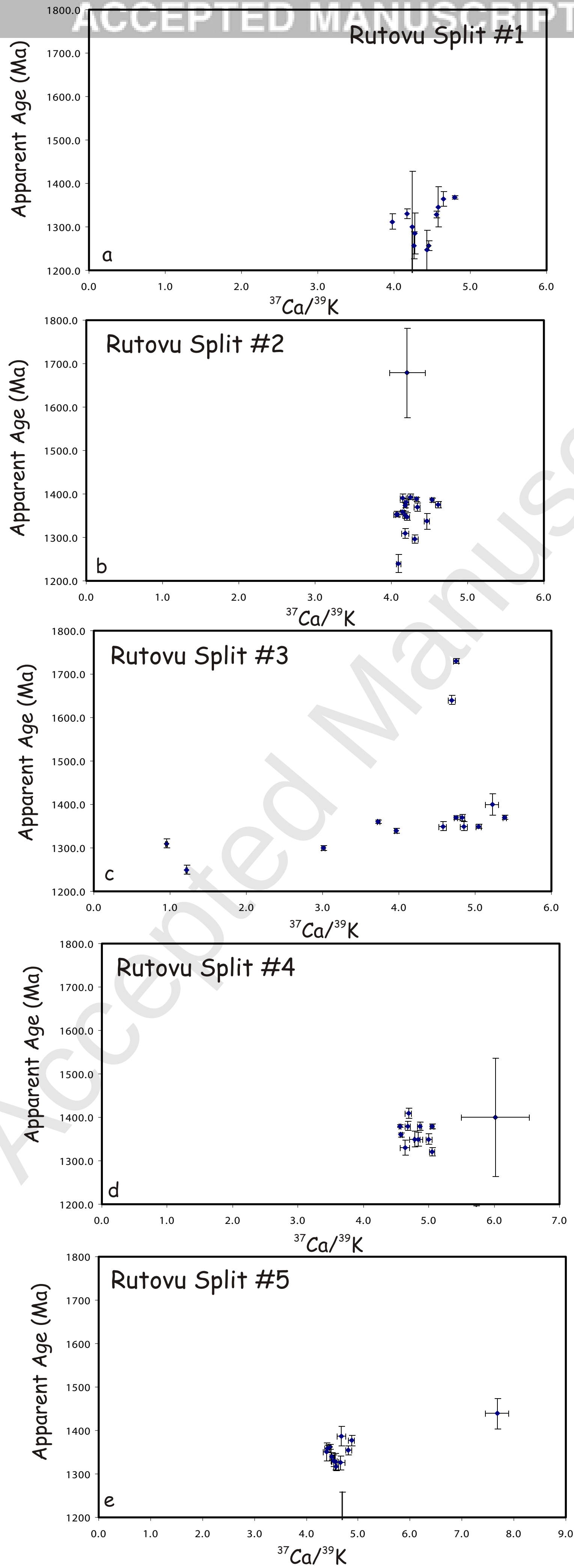
Rutovu Split #1
a
Rutovu Split #2
b
Rutovu Split #3
c
Rutovu Split #4
d
Rutovu Split #5
e
Apparent Age (Ma)
$^{37}Ca/^{39}K$
1800.0
1700.0
1600.0
1500.0
1400.0
1300.0
1200.0
0.0
1.0
2.0
3.0
4.0
5.0
6.0
7.0
8.0
9.0

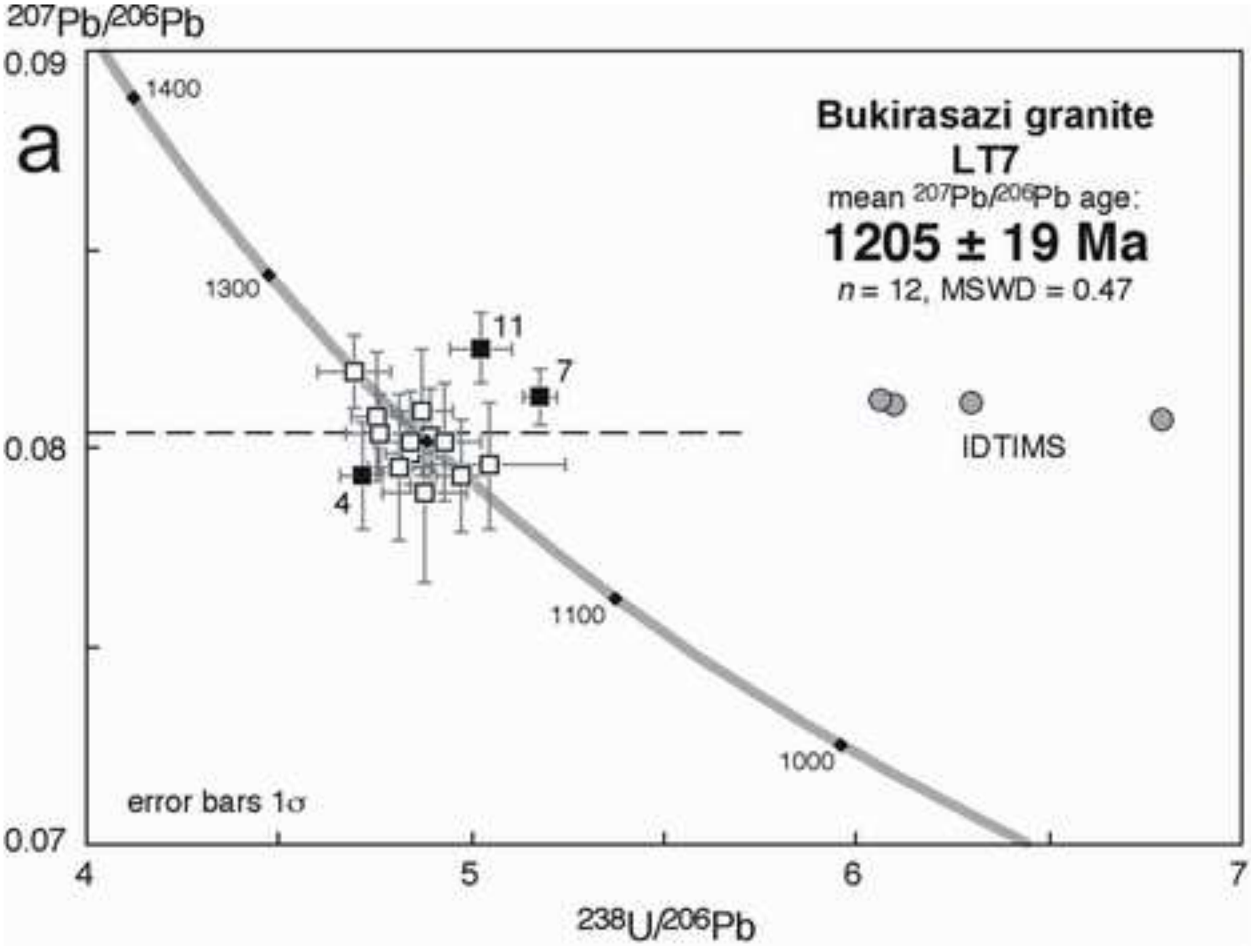

a
Bukirasazi granite
LT7
mean $^{207}Pb/^{206}Pb$ age:
1205 ± 19 Ma
$n$ = 12, MSWD = 0.47
IDTIMS
error bars 1σ
$^{207}Pb/^{206}Pb$
$^{238}U/^{206}Pb$
1400
1300
1100
1000
11
7
4
0.09
0.08
0.07
4
5
6
7


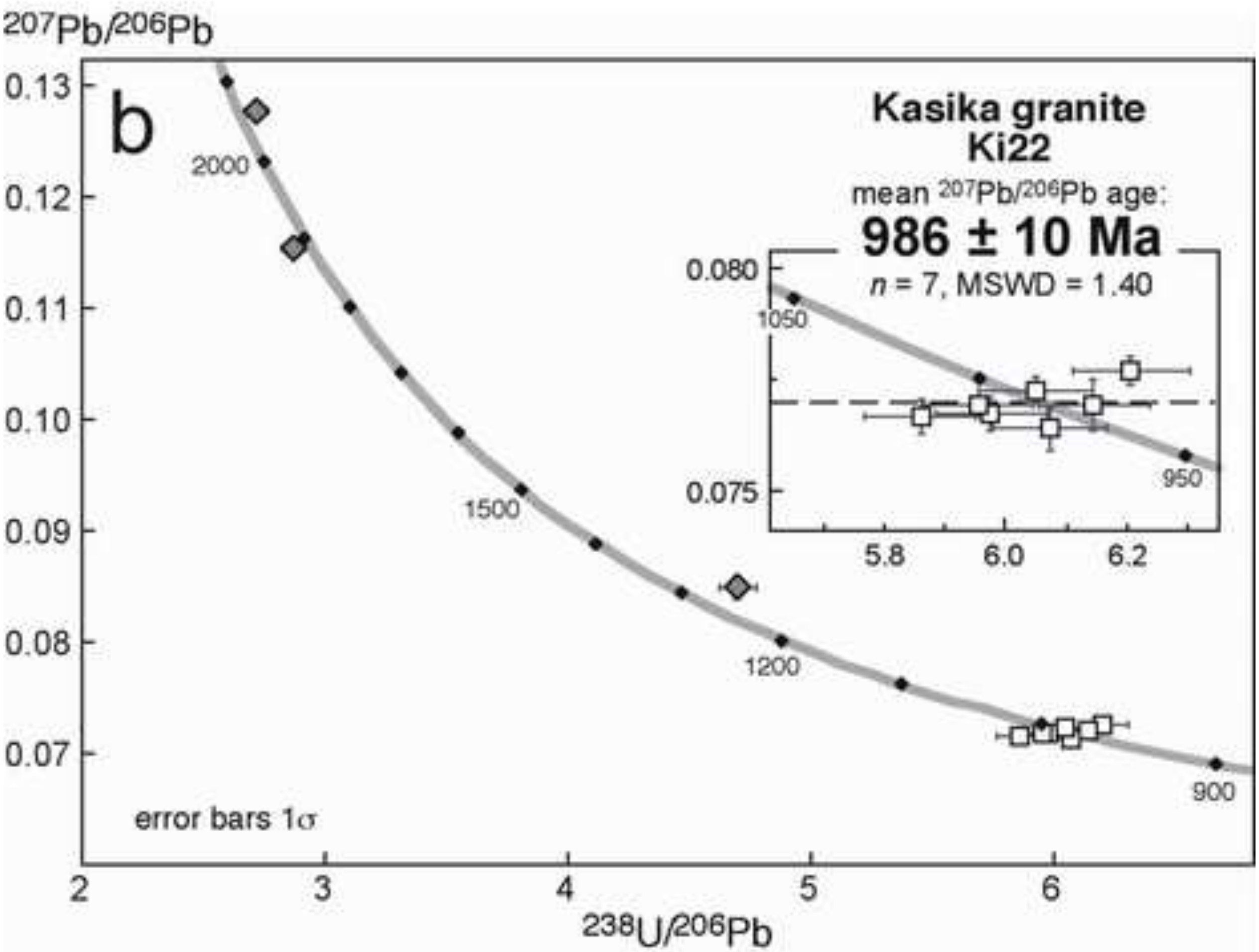

b
Kasika granite
Ki22
mean $^{207}Pb/^{206}Pb$ age:
986 ± 10 Ma
$n$ = 7, MSWD = 1.40
error bars 1σ
$^{207}Pb/^{206}Pb$
$^{238}U/^{206}Pb$
2000
1500
1200
900
1050
950
0.080
0.075
5.8
6.0
6.2
0.13
0.12
0.11
0.10
0.09
0.08
0.07
2
3
4
5
6

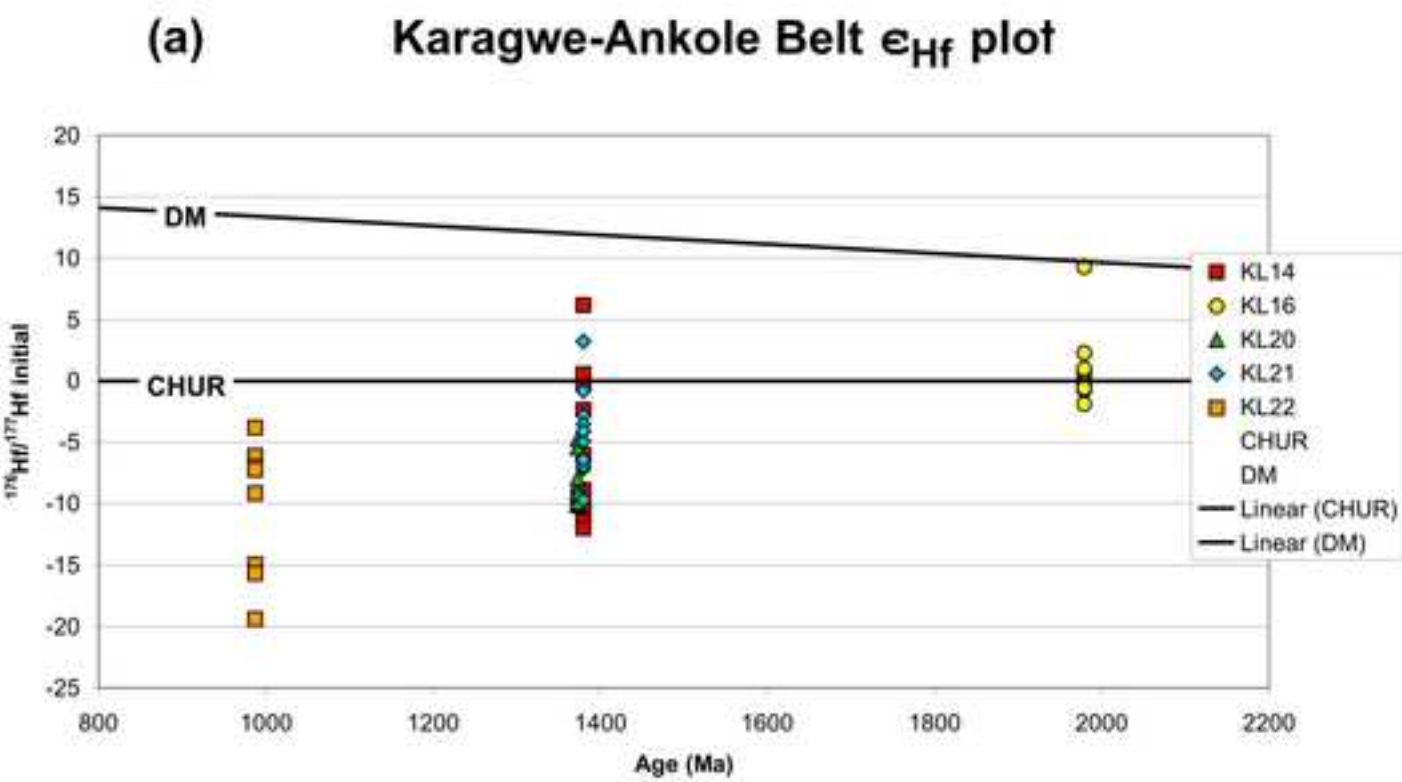
(a)
Karagwe-Ankole Belt $\epsilon_{Hf}$ plot
DM
CHUR
$^{176}Hf/^{177}Hf$ initial
20
15
10
5
0
-5
-10
-15
-20
-25
800
1000
1200
1400
1600
1800
2000
2200
Age (Ma)
KL14
KL16
KL20
KL21
KL22
CHUR
DM
Linear (CHUR)
Linear (DM)

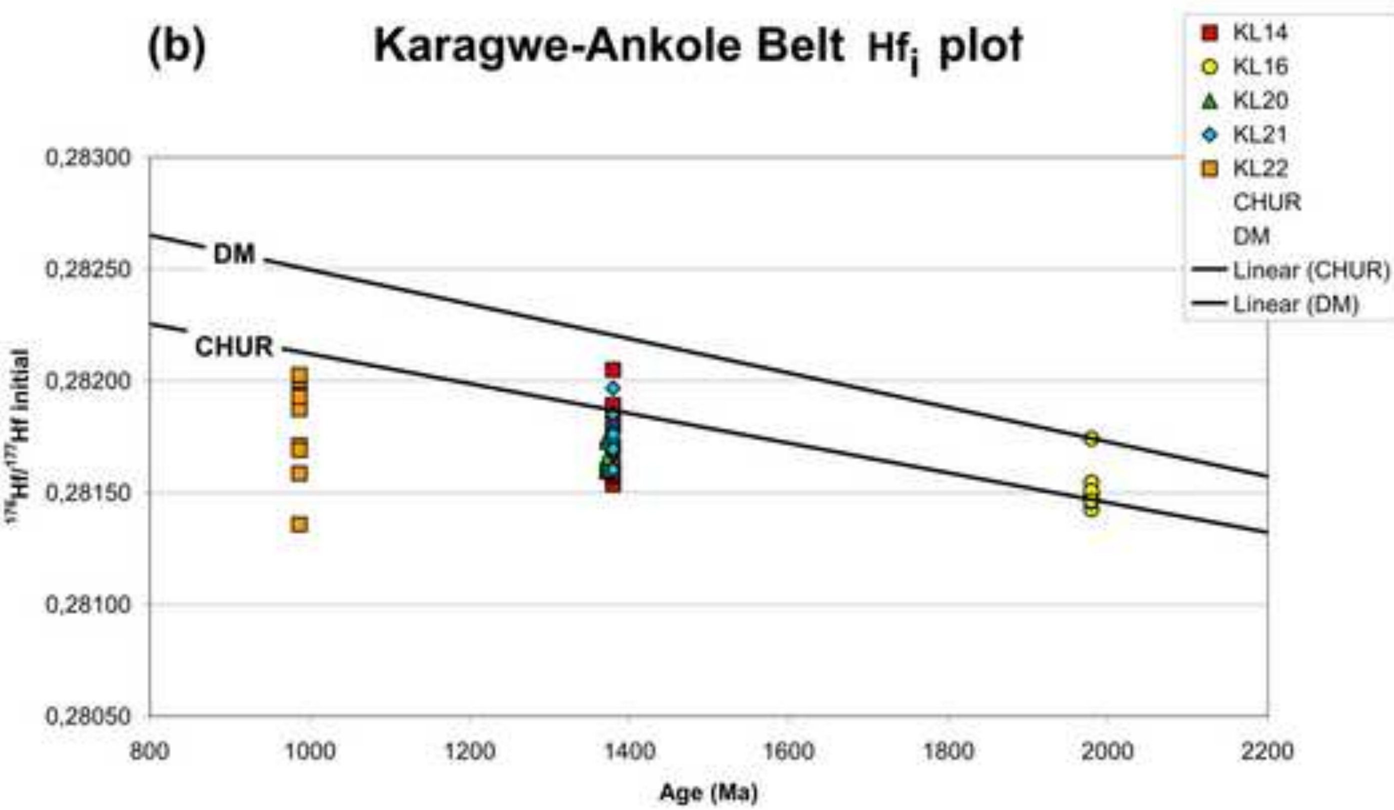
(b)
Karagwe-Ankole Belt $Hf_i$ plot
DM
CHUR
$^{176}Hf/^{177}Hf$ initial
0,28300
0,28250
0,28200
0,28150
0,28100
0,28050
800
1000
1200
1400
1600
1800
2000
2200
Age (Ma)
KL14
KL16
KL20
KL21
KL22
CHUR
DM
Linear (CHUR)
Linear (DM)

Table1



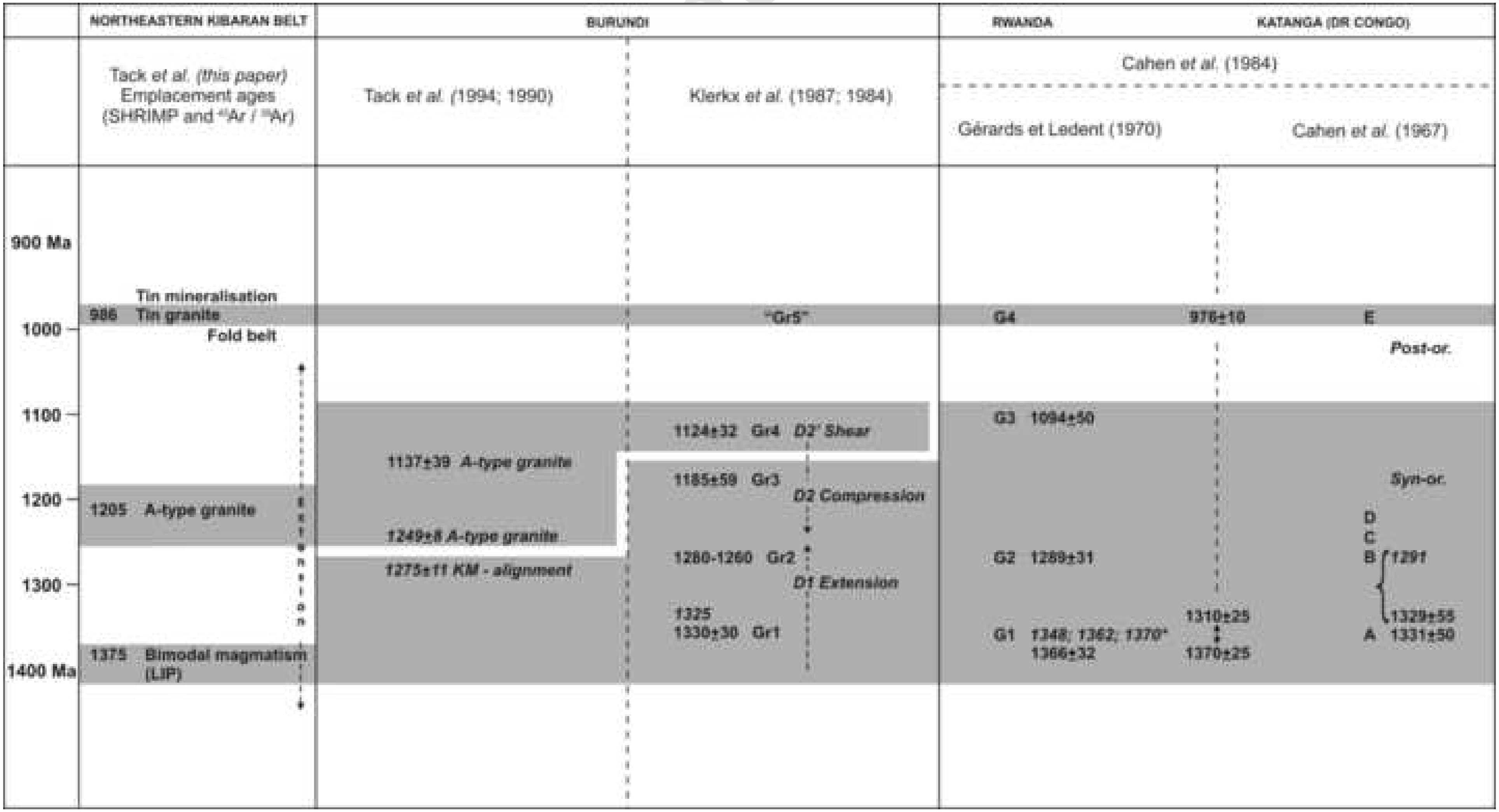
NORTHEASTERN KIBARAN BELT
BURUNDI
RWANDA
KATANGA (DR CONGO)
Tack et al. (this paper)
Emplacement ages
(SHRIMP and 40Ar / 39Ar)
Tack et al. (1994; 1990)
Klerkx et al. (1987; 1984)
Cahen et al. (1984)
Gérards et Ledent (1970)
Cahen et al. (1967)
900 Ma
1000
1100
1200
1300
1400 Ma
Tin mineralisation
986 Tin granite
Fold belt
1205 A-type granite
1375 Bimodal magmatism
(LIP)
extension
"Gr5"
1137±39 A-type granite
1249±8 A-type granite
1275±11 KM - alignment
1124±32 Gr4 D2' Shear
1185±59 Gr3
D2 Compression
1280-1260 Gr2
D1 Extension
1325
1330±30 Gr1
G4
976±10
E
Post-or.
G3 1094±50
Syn-or.
D
C
B 1291
G2 1289±31
1310±25
1370±25
1329±55
G1 1348; 1362; 1370*
1366±32
A 1331±50

Table2



| Serial number (Fig. 5) | Sample number (this paper) | Locality name and previous classification | New isotopic ages (Ma) (this paper) | Previous "age" data (Ma) | RG-number of RMCA (Tervuren) sample collection |
|---|---|---|---|---|---|
| 1 | Ki 16 | Butare pre-Kibaran basement | 1982 ± 6 | 1920 (2) | 71177 |
| 2 | 63,865 | Rumeza Gr 1; S-type | 1383 ± 17 | 1370 (2)<br>1335 ± 25 (10) | 63865 |
| 3 | Ki6684 | Mugere Gr 2; S-type | 1379 ± 10 | 1261 ± 25 (4) | 141979 |
| 4 | Ki21 | Mugere migmatitic paragneiss | 1380 ± 12 | | 160906 |
| 5 | Ki1 | Kiganda Gr 3; S-type | 1371 ± 7 | 1185 ± 59 (4) | 161566 |
| 6 | Ki14 | Muramba S-type | 1380 ± 6 | 1324 ± 23 (8)<br>1279 ± 65 (4) | 144875 |
| 7 | Ki20 | Kilimbi-Muzimu S-type | 1373 ± 6 | 1111 ± 39 (9) | 145716 |
| 8 | DB1 | Musongati amphibole norite | 1374 ± 14<br>1365 ± 2 (*) | 1275 ± 11 (5) | 161332 |
| 9 | A114 | Rutovu hornblende granophyre | 1368 ± 18 (*) | | 155535 |
| 10 | LT7 | Bukirasazi "Gr 4"; A-type | 1205 ± 19 | 1249 ± 8 (5)<br>1137 ± 39 (6)<br>1124 ± 32 ; 1125 ± 25 (4) | 155479 |
| 11 | Ki22 | Kasika tin granite | 986 ± 10 | 976 ± 10 (2;7) | 71157 |

| | | | | | |
|---|---|---|---|---|---|
| | | | | 951 ± 12 (7) | |
| 12 | Mo92 | "Kavumwe" mafic sill | 1360 ± 20 (*) (1)<br>1340 ± 9 (*) (1) | ca. 1010 (2) | 161280 |
| 13 | Mo89 | "Bukoba Sandstone" mafic sill | 1379 ± 10 (*) (1)<br>1355 ± 10 (*) (1) | 812 ± 30 (3)<br>815 ± 30 (3) | 161278 |

**Table 3**

*Sample location and characteristics of zircons in samples from the Karagwe-Ankole belt (KAB)*

| Sample | Size (μm) | Aspect ratio | Shape | Clarity | Colour | Character in cathodoluminescence images | Interpretation |
|---|---|---|---|---|---|---|---|
| Ki16 | 50-350 | 1:1 - 3:1 | Euhedral | clear to turbid | yellow to dark brown | Concentric oscillatory zoning; some homogeneous dark-CL rims | Magmatic zircon. High-U rims are probably late-magmatic, but possibly metamorphic |
| 63.865 | 50-300 | 1:1 - 3:1 | Sub- to euhedral | clear to turbid | colourless to dark brown | Concentric oscillatory zoning | Magmatic zircon |
| Ki6684 | 100-600 | 1:1 - 6:1 | Euhedral | clear | pale brown | Concentric oscillatory zoning; some rounded cores | Magmatic zircon; some inherited cores |
| Ki21 | 100-300 | 1:1 - 5:1 | Euhedral | clear | colourless to pale yellow | Concentric oscillatory zoning; some zoned irregular cores with dark zoned rims | Magmatic zircon; some inherited cores |
| Ki1 | 100-500 | 2:1 - 6:1 | Euhedral | clear to opaque | pale brown to dark brown | Concentric oscillatory zoning; some zoned or unzoned cores | Magmatic zircon; some inherited cores |
| Ki14 | 100-200 | 1:1 - 5:1 | Euhedral | clear | colourless to pale yellow | Concentric oscillatory zoning; some zoned or unzoned cores | Magmatic zircon; some inherited cores |
| Ki20 | 100-500 | 1:1 - 3:1 | An- to euhedral | clear to turbid | colourless to dark brown | Concentric oscillatory zoning, truncated by younger rims | Magmatic zircon with metamorphic rims |
| DB1 | 40-100 | 1:1 - 3:1 | Sub- to euhedral | clear | colourless | Concentric oscillatory zoning | Magmatic zircon |
| LT7 | 100-200 | 1:1 - 3:1 | Sub- to euhedral | clear to opaque | colourless | Concentric oscillatory zoning | Magmatic zircon |
| Ki22 | 100-350 | 1:1 - 3:1 | Sub- to euhedral | clear to turbid | colourless to dark brown | Concentric oscillatory zoning; some dark-CL rims; mottled and irregular textures common | Magmatic zircon; possibly younger rims |